Institut für Werkstoffe der Energietechnik

Performance of HTR Fuel Samples under High-Irradiation and Accident Simulation Conditions, with Emphasis on Test Capsules HFR-P4 and SL-P1

W. Schenk R. Gontard H. Nabielek

Performance of HTR Fuel Samples under High-Irradiation and Accident Simulation Conditions, with Emphasis on Test Capsules HFR-P4 and SL-P1

W. Schenk R. Gontard H. Nabielek

Abstract

The central aspect of the safety philosophy for a small HTR is the retention of fission products, particularly those of the iodine nuclides, in the fuel elements during operation and accidents. The HFR-P4 and SL-P1 experiments were intended to test the performance limits of the LEU TRISO particle during irradiation. Due to the low heavy metal contamination of modern fuel elements, fission gas or iodine release is dominated by the number of defective coated particles. For this reason, the determination of the number of damaged particles was the central objective of measuring the fission gas releases in the reactor and in the extensive post-irradiation examinations. Although the values for burnup, fast neutron fluence and irradiation temperature envisaged in an HTR-MODUL were clearly exceeded, it became apparent that of a total of 78,400 particles employed, only one was defective (i.e. not gastight) during irradiation. In which connection, the damage probably occurred before irradiation, at the end of pre-activation treatment. Two further incidences of particle damage probably occurred during shutdown of the HFR-P4 experiment.

During the 300 h heating experiments at 1600°C and 1700°C, no particle defects occurred in seven compacts within the temperature/time conditions characteristic of a MODUL depressurization accident. In the case of the compacts with 14 % burnup at 1600°C and 10 or 11 % burnup at 1700°C, the release of fission gas started to rise after 47 to 135 hours to about 0.01 % at the end of the experiment, and in one case to 0.1 % as the consequence of one failed particle. Only in the 1800°C experiment did the Kr release rise continuously, but still only reached 0.01 % after 150 hours. During the heating experiments the fission products were released in sequence fission gases, iodine, strontium, caesium and, with the highest proportion, silver, which is of little significance for accident consequences. Due to their transport and deposition behaviour in the core, caesium and strontium release, is insignificant for MODUL accident impacts. After 300 hours at 1600°C, more than 99 % of the caesium is still in the coated particles. However, considerable release begins with increasing heating temperature amounting to about 50 % from the compact at 1800°C after 280 h. Strontium is more effectively retained in the fuel kernels and matrix graphite at 1600°C than caesium . At 1700 and 1800°C, the strontium release approaches that of caesium.

All these tests, containing in total the equivalent number of particles of 5 fuel elements, show that - even after more severe irradiation conditions than those envisaged during HTR MODUL operation - no particle failures occured either during operation or during severe accident conditions.

Index Page

1. **Introduction** 1

2. **Justification and Objectives** 5

3. **Sample Fabrication** 8
   - 3.1 Fabrication of the low-enriched UO2 fuel kernel 8
   - 3.2 Coating manufacture 10
   - 3.3 Compact fabrication 14

4. **Irradiation** 16
   - 4.1 Irradiation devices 16
   - 4.1.1 HFR-P4 irradiation insert 18
   - 4.1.2 SL-P1 activation test 20
   - 4.1.3 Irradiation insert SL-P1 20
   - 4.2 Irradiation target values 21
   - 4.3 Irradiation results 23
   - 4.3.1 HFR-P4 irradiation results 24
   - 4.3.2 SL-P1 irradiation values 26

5. **Post-irradiation examination** 27
   - 5.1 Disassembly, dimension measurements and cold gas test 28
   - 5.2 Gamma spectrometry for determining the neutron flux, fission product inventory and burnup 29
   - 5.3 Hot gas chlorination 34
   - 5.4 Comparison of the particle defects determined by various methods 35

6. **Accident Simulation Tests** 39
   - 6.1 Procedure 40
   - 6.2 Sample data 43
   - 6.3 Release from the compacts at 1600 to 1800°C 45
   - 6.4 Fission product fraction in the matrix graphite 53
   - 6.5 Fission product transport and changes in particles 55
   - 6.6 Summarizing evaluation of the results 63

7. **Conclusions** 67

8. **References** ..... I-VIII

Index of abbreviations used

HTR	High-temperature reactor
MODUL	HTR with 20 MW thermal
PNP	HTR prototype nuclear process heat
MTR	Material test reactor
AVR-Jülich	Arbeitsgemeinschaft Versuchsreaktor - Jülich
NUKEM	German fuel manufacturer
KFA Jülich	Research Centre Jülich
HZ	Hot Cell laboratory
OEFZS	Austrian Research Centre, Seibersdorf - Austria
AERE	Atomic Energy Research Establishment, Harwell
GA	General Atomics, San Diego

Descriptions of particles

C.P.	Coated particle
PyC layer	Particle coating of pyrocarbon
BISO coating	Particle coating of several different pyrocarbon layers
TRISO coating	Particle coating of pyrocarbon layers with an additional SiC intermediate layer
HTI	High temperature isotropic (PyC form methane)
LTI	Low temperature isotropic (PyC from propene or propene/ethine)
HEU	High-enriched uranium
LEU	Low-enriched uranium

Designations of fuel elements

GLE	Fuel elements with low-enriched UO_2 particles (AVR)
FRJ 2-K	Fuel elements irradiated in the Jülich Dido reactor
HFR-P	Samples with particles irradiated in material test reactor HFR in Petten, the Netherlands
SL-P	Samples with particles irradiated in material test reactor SILOE in Grenoble

1. Introduction

The design of modern HTRs is based on high-quality fuel.
The very good retention of radiologically significant fission products by TRISO-coated particles has been studied extensively in the German fuel development programme. The high degree of safety of HTRs results from the ability of coated fuel particles to retain fission products even at high temperatures.

Small modular HTRs are designed in such a way that maximum fuel temperatures during severe accidents remain below 1600°C without active control mechanisms /1/. This temperature limit is based on thermodynamic calculations for proposed MODUL designs. The temperature limiting features have been demonstrated in reactor experiments, e.g. those in the Jülich AVR reactor /2,3,4/.

The 1600°C temperature limit in the modular HTR is achieved by a core design with a thermal power of 200 MWth and a low power density, 3 MW/m^3. In the tall and slim core, the heat is transported away during a loss-of-coolant accident by passive means, i.e. by radiation and conduction. Also, the reactor design places very modest requirements on fuel and graphite during normal operation. Irradiation temperatures are 700-900°C, the target burnup is 9% FIMA and the accumulated fluence of fast neutrons is $2.1 \times 10^{25}\ m^{-2}$.

The maximum fuel temperature during uncontrolled core heatup is 1150°C in a pressurized system. For a complete loss of coolant, a nominal maximum temperature of 1520°C is attained in a small portion of the core /5/. When all calculational uncertainties are added up in a conservative manner, the peak core temperature may rise to 1620°C in 30 hours. Most accident simulation tests have been conducted at constant 1600, 1700 and 1800°C for much longer times than expected to determine the performance margins of the fuel system.

The development of the coated particle over more than 10 years led to the modern UO_2 TRISO type /6/. The coated particle in HTR fuel elements is at the heart of the design of a high-temperature reactor. Figure 1 illustrates a fuel element and a coated particle. The coatings withstand the pressure from fission gases generated during burnup, and provide a barrier that retains all radiologically significant fission products during normal operations and during extreme accidents.

The production of spherical fuel elements for HTRs consists of the following steps:

- fuel kernel formation;
- coating of microspheres;
- matrix powder preparation;
- overcoating of particles;
- fuel element fabrication, i.e. pre-moulding of fuel zone, high-pressure isostatic pressing of complete element, machining, and 900 / 1950°C heat treatment; and
- quality control.

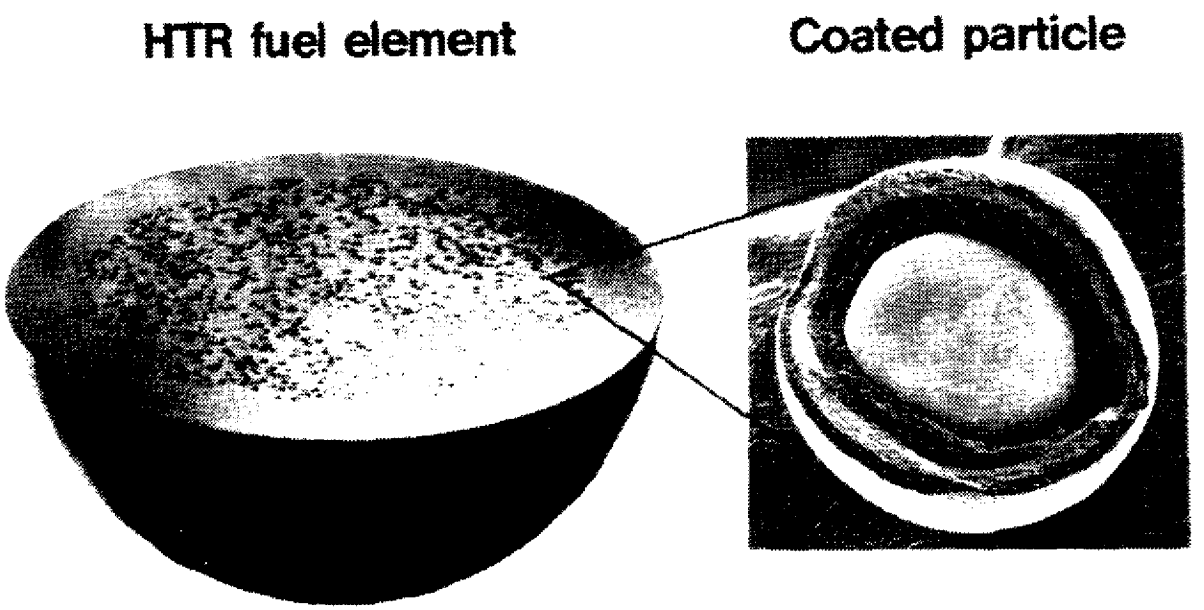

Fig. 1: Section through 60 mm-diam. fuel sphere and view of 0.9 mm-diam. particle with part of the coating removed

Within the 60 mm diameter spherical fuel element, the fuel is discretely dispersed in 16,400 coated particles. Their TRISO particles have a 500 µm diameter UO_2 kernel with 10% ^{235}U enrichment and a 200 µm thick coating, consisting of a porous buffer layer and two dense layers of pyrocarbon with a silicon carbide layer in between (Fig. 2). While all these layers have important mechanical and chemical functions, it is the SiC which guarantees the highest degree of fission product retention.
In normal and transient operation, and in accidents not exceeding 1600-1700°C, it can be demonstrated that all radiologically relevant fission products (iodine, caesium, strontium) are completely retained inside the silicon carbide layer of intact fuel particles. The dominant source term of fission product release will, therefore, be the small number of particles with defective coatings /7,8/.

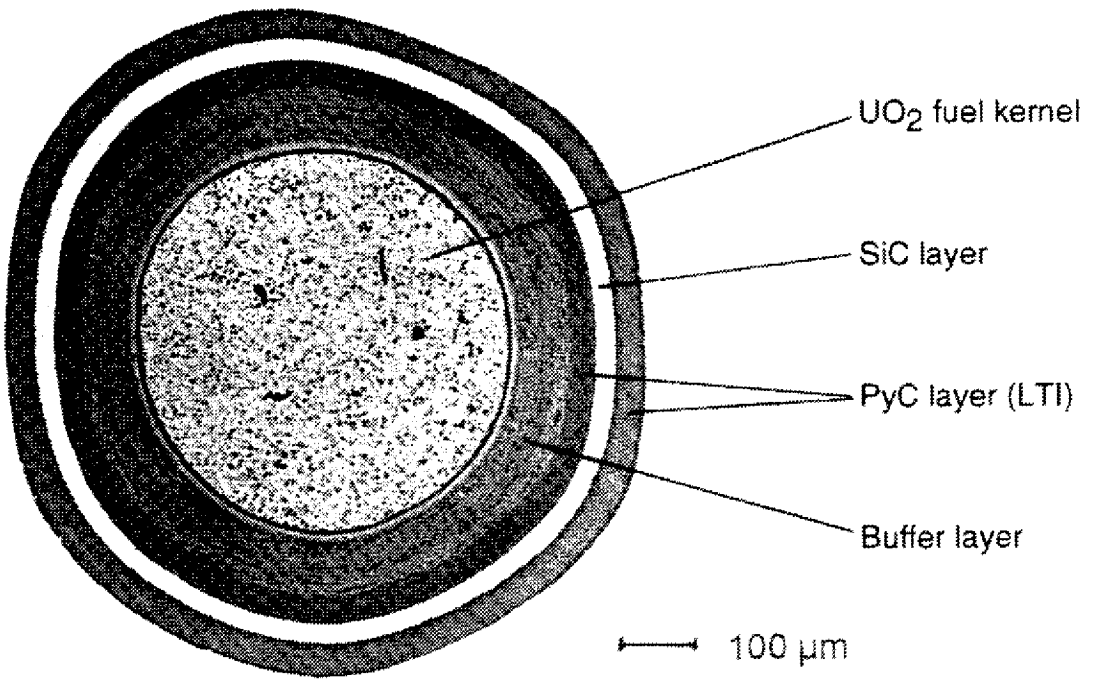

Fig. 2: Cross-section through an LEU TRISO coated particle

The content of free uranium in fuel elements with TRISO particles is determined by the burn-leach method /7/. This quality control procedure measures the "free" uranium as uranium sources not contained by intact silicon carbide coatings. These are:

- uranium contamination of the fuel element matrix and the outer pyrocarbon of the particles;
- particles with completely broken coatings; and
- particles with micro-cracks in the SiC but intact PyC layers.

The measured values of the total free uranium fraction within spherical fuel elements containing UO_2 TRISO particles cover a range between 8 and 51×10^{-6}. Conservatively, the defect fraction 30×10^{-6} had been chosen /8/ as an expected value for future fuel element production. The more important design value, on which all radiological calculations are based, has been fixed at 60×10^{-6}.

Under the management of the Research Centre Jülich, a number of fuel performance and fission product behaviour irradiation experiments were initiated in Euro-

pean MTRs and three large-scale demonstration charges were introduced into the AVR in the time period from 1981 through 1987. The irradiation programme consisted of a number of tests all of which, except the AVR real-time demonstration charges, were conducted in purged experimental capsules /9/.

The fuel elements in these experiments had modern UO_2 TRISO particles fabricated by NUKEM in 1981. The in-reactor performance of these fuels, with follow-on post-irradiation examinations and fission product release analyses, and post-irradiation accident simulation tests, have demonstrated a high level of fuel performance of the reference UO_2 system /10/.

Three experiments with four spheres each were irradiated in the High Flux Reactor in Petten (HFR-K3, -K5 and -K6) and two experiments with four or three fuel spheres in the Jülich DIDO reactor (FRJ 2-K13 and -K15). Beginning in July 1982 more than 50,000 fuel elements with UO_2 TRISO particles were charged into the AVR core /10/. Additional cylindrical compacts were manufactured from initially spherical fuel elements having a small fuel zone, these were inserted into the three HFR-P4 experiments and one Siloe experiment in Grenoble (SL-P1). The results of these experiments are described in this report.

During irradiation, there was continuous monitoring of released fission gases, indicating the integrity of particle coating. It was concluded that no irradiation-induced particle failure occurred in any of the irradiation tests containing modern TRISO fuel /11, 12/.

In addition to the analysis of fission gas release, non-destructive and destructive post-irradiation examination (PIE) techniques are applied. The first PIE step is the disassembly of capsules with subsequent examination of their components; fuel samples, graphite bodies and capsule steel tube by visual methods, dimensional measurements and by gamma spectroscopy.

Gamma spectrometry of the fuel provides data on the burnup, the contribution of plutonium fissions to total burnup and the inventory of fission products. Gamma spectrometry of the components outside the fuel body yields the release of long-lived metallic fission products like ^{137}Cs, ^{134}Cs, ^{110m}Ag, ^{154}Eu /13/. Fractional caesium releases as measured with PIE at the level of 10^{-5} of the fuel inventory are, however, around the limit of detection in hot cell work and, as a result, may not necessary be correlated with irradiation parameters and with fuel performance predictions.

^{110m}Ag release becomes noticeable in irradiation tests >1000°C and ^{137}Cs at irradiation temperatures >1300°C.

Selected irradiated fuel spheres and other fuel samples are subjected to accident simulation heating tests at 1600°C, 1700°C and 1800°C in an apparatus that enables determination of the release of gaseous and condensible fission products /14/. When accident temperatures are limited to less than 1600°C for expected accident times, the heating data confirm that reactor licensing applications can be based on 1 coated particle failure in 4 fuel elements and no additional release of safety-relevant fission products, especially iodine, beyond that associated with normal operation.

2. Justification and Objectives

Relative recent evaluation of various fuel cycles in high-temperature reactors led to the decision to employ low enriched uranium as the initial fuel /15/. As indicated in Fig. 3., the HTR concept previously use the mixed thorium-uranium cycle initially fueled with (Th, U) O_2.

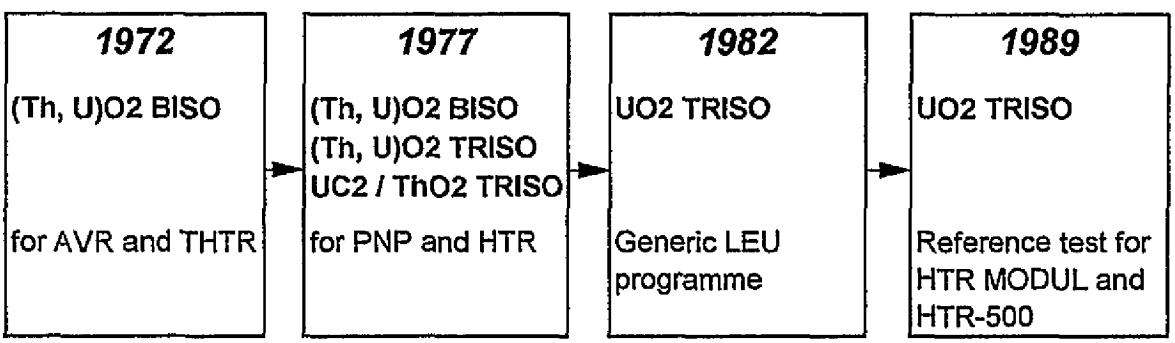

Fig. 3: German fuel particle development carried out a function of time

For HTR particle development, the decision to use LEU fuel means the resumption of work on low-enriched UO_2 kernels with TRISO coating that has been discontinued in 1973. Existing fabrication and irradiation experience was included in considerations concerning the design of the kernel and coating. Evaluation tests to cover a wide range of particle varieties were therefore not necessary.

All planned irradiation experiments were to be carried out with the same fuel in order to obtain reliable information as quickly as possible about the irradiation behaviour of the LEU particles of the first "Standard Quality" fabricated at HOBEG in the first six months of 1981.

An extensive fuel irradiation test program was carried out to determine the performance of LEU UO_2 TRISO coated particles. Table 12 gives a summary of the test parameters and irradiation results obtained from all tests carried out in Material Test Reactors. In addition, irradiated fuel compacts were selected and exposed to post-irradiation high-temperature-heating conditions. Finally, selected AVR fuel elements irradiated in the AVR were exposed to post-irradiation high temperature. Fuel performance as measured by fission product retention within the coated particles and within fuel compacts/elements were determined experimentally.

LEU TRISO particles that still resulted in very high fuel performance (the latter implies very high retention of radiologically significant fission products within fuel compacts/elements)/16/17/.
To qualify a particle design for use in HTR's, determination of the irradiation induced failure of the fuel coatings is the most important prerequisite for a licensable fuel element specification. In addition, it is important to determine the influence of temperature on particle failure and on failure mechanisms.
Particularly in the case of determining the limits of irradiation and other test conditions that still give high fuel performance, the actual test temperatures must be precisely determined and spurious temperature gradients must be avoided.

The sample shape envisaged for HFR-P4 and SL-P1, namely cylindrical compacts with a spherical fuel zone, offers a good opportunity of inserting a number of thermocouples in boreholes in the matrix of the fuel-free zone surrounding the fuel. The thermocouples are distributed throughout the entire height of the compact stack and thus ensure a temperature profile that can be determined all over the capsule. Temperature gradients are controlled by a suitable choice of gas gaps, that control heat transport.

Particles with UO_2 fuel and LTI-TRISO coating were selected as the reference fuel for the spherical HTR fuel elements in the LEU cycle. In designing the particle, particular care was taken that the geometry of the tested HEU particle with a mixed oxide fuel kernel /18/ should be matched as closely as possible in order to avoid unnecessary new developments and additional irradiation tests. Analogous to the HEU particle, the fuel kernel has a diameter of 500 µm; the pyrocarbon coatings are

also adapted from HEU design with a buffer layer of 90 µm and an inner and outer PyC layer of 40 µm respectively. There was still some uncertainty about the design of the SiC layer. Due to the different range of fission products, a different chemical interaction between the fission products and the SiC layer was assumed for a LEU kernel than in the case of an HEU kernel. In experiment HFR-P4, a particle variant with a SiC layer of 51 µm was therefore selected instead of the 36 µm layer otherwise used.

To estimate the consequences of increasing the SiC coating thickness on mechanical strength of the particles, stress calculations were carried out at the Institute for Materials in Energy Systems at the KFA using the stress model /19/. These calculations indicate that reinforcing the SiC layer would reduce the failure fraction by half an order of magnitude. However, the failure fraction would be reduced by four orders of magnitude with a buffer layer increased by 30 %, and also by two orders of magnitude if the standard deviation of the buffer layer thickness was reduced, by half.

Summary of Objectives of Test Capsules HFR-P4 and SL-P1 and associated Test Conditions

HFR-P4	SL-P1
Overall Objectives	
Determination of particle failure of LEU reference particles during irradiation	
Fuel Performance for Irradiations BEYOND potential reactor burnup and fast fluence	Fuel Performance for Irradiations UP TO potential reactor burnup and fast fluence
Comparison of fuel performance of coated particles having SiC thicknesses of 36 µm and of 51 µm	Determine irradiation level that causes particles coatings to start to fail

HFR-P4

Temperature

Design	*Actual*
1000/1200°C	940/945/1075°C

Burnup and fluence

9% FIMA 2.2 E+25n/m²	4.0-14.9% FIMA 8.0 E+25n/m²
(E>16 fJ)	

SL-P1

Design	*Actual*
800°C	800°C

9% FIMA 2.2 E+25n/m²	9% FIMA 5.0-6.8 E+25n/m²
(E>16 fJ)	

3. Sample Fabrication

The methods used in the previous fabrication of HEU-TRISO mixed oxide particles were largely employed in producing the kernels and coatings, but were modified slightly/20, 21/.

3.1 Fabrication of the low-enriched UO_2 fuel kernel

Starting from U_3O_8 powder, the powder is dissolved in nitric acid thus forming uranyl nitrate. After adding organic agents. THFA and neutralizing with ammonia, the solution flows through vibrating nozzles and is transformed into droplets.

Falling through a gaseous ammonia atmosphere the droplets attain a distinct oxide surface before dipping into the aqueous ammonia solution. In the solution, these small spheres will solidify by forming ammonium uranate. Subsequently, the droplets are aged to improve their internal structure by remaining in the warm ammonia solution for some time and then being washed to remove the ammonium nitrate and organic additives. This is followed by drying, calcining, reduction to UO_2 with hydrogen and, finally, sintering to produce kernels of 98 % theoretical density (Fig. 4).

Development work concentrated on testing the possibility of employing the Gel precipitation method to fabricate 500 µm UO_2 kernels. Several process steps greatly influencing the kernel quality had to be modified:

- pouring solution
- ageing and
- sintering.

After producibility had been demonstrated, the altered parameters were laid down and documented in a laboratory quality. The essential parameters of the Gel precipitation method for kernel fabrication are described in /22/.

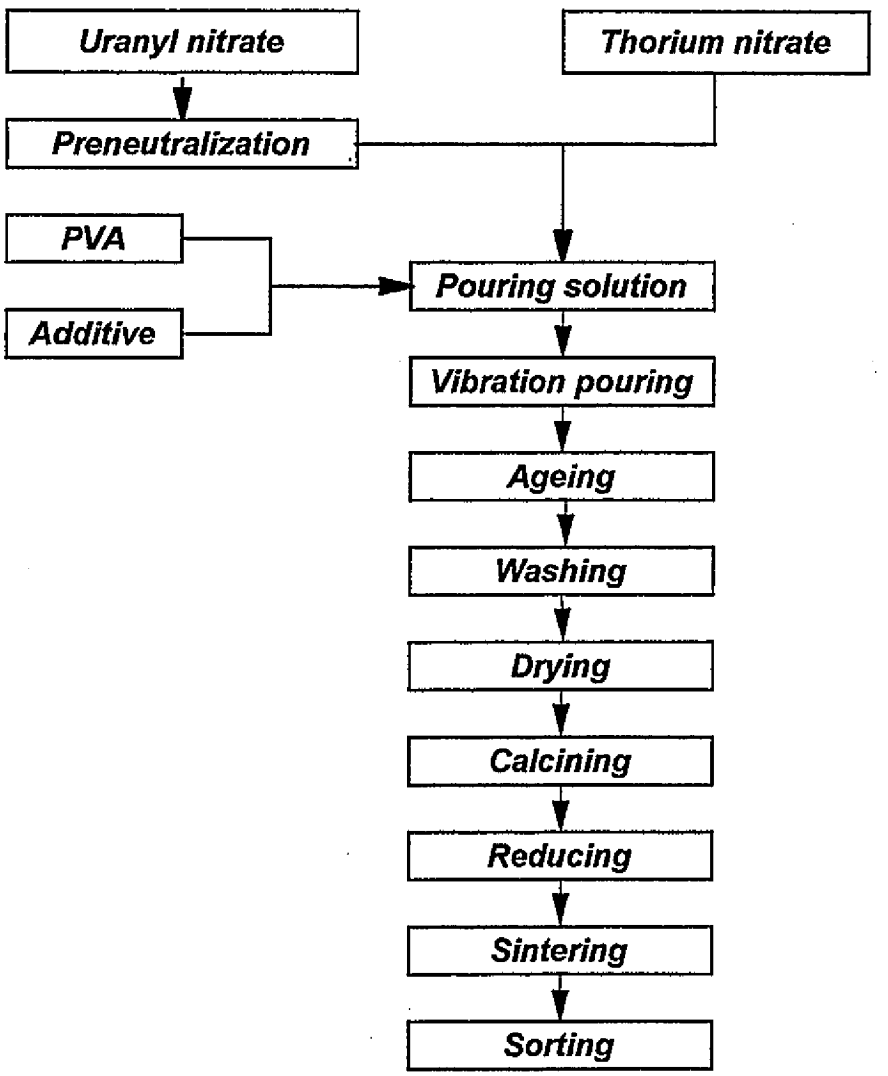

Fig. 4: Flow chart: Production of UO_2 kernels

The revised process for fabrication of UO_2 fuel kernels proceeds according to the following steps:

The initial solution (uranyl nitrate) is preneutralized with aqueous ammonia solution. After the addition of organic agents, the pouring solution is introduced into a three-nozzle facility and the emerging droplets first aged in hot water at 50°C. This is followed by a washing process at room temperature, first in water and then in isopropanol. After the kernels have been dried in a partial vacuum, they are calcined at 300°C in air. Reduction under Ar/H_2 is then carried out at 600°C. The kernels are ultimately sintered to their final density at 1650°C under H_2. The kernels were characterized and divided into representative coating batches of 5 kg each.

3.2 Coating manufacture

Coating is carried out by passing a stream of carrier gas (argon and/or hydrogen) upwards through a batch of 5 or 10 kg of kernels so that they form a fluidized bed. The bed is kept at a controlled high temperatures in the furnace. Various organic gases are added to the fluidizing gas in subsequent steps (Fig. 5). By chemical vapour decomposition (CVD) of these compounds, carbon or silicon carbide will be deposited. The coating gas agents for the buffer and PyC (pyrolytic carbon) layers are hydrocarbons and methyl trichlorosilane for the silicon carbide.

The properties of the coatings are dependent on the composition of the added gases, as well as on temperature and flow rate. The diameter of the coated fuel spheres will increase during growth of the layers and the average density will decrease. Adjustment of the flow rate is used to keep the coated particles in a fluidized condition. The different layers are deposited consecutively without interrupting the process or discharging until all the layers have been deposited.

The procedure for coating mixed oxide (Th, U) O_2 kernels was essentially taken over for particles with a 35 µm SiC layer. However, attention had to be paid to the relevant properties of UO_2 versus that of Th O_2, such as the

- approximately 8 % higher kernel density of UO_2
- higher chemical reactivity, of UO_2 with carbon

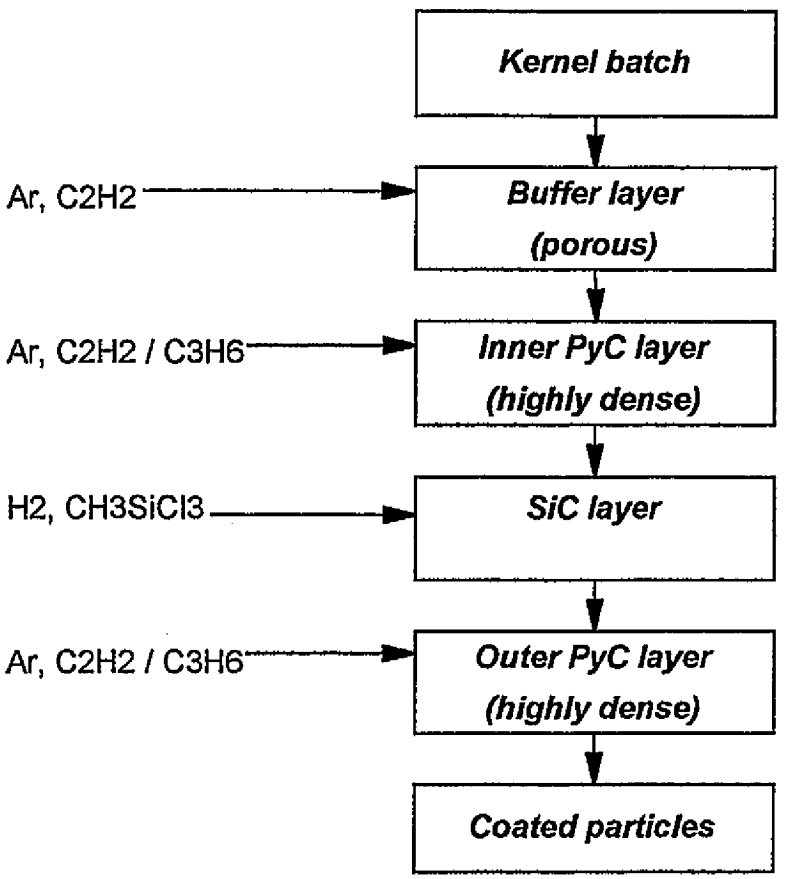

Fig. 5: Coating sequence of HTR fuel particles

Studies of the chemical reactivity of UO_2 with carbon during the coating process indicated that no reaction took place between the kernel material and pyrocarbon layer. Nor did sintering of the coated particles at 1950°C reveal any reaction zones in the ceramographic section. The layer properties correspond to those of the previously fabricated (Th, U)O_2 and ThO_2 particles.

In order to produce the particles with a 50 µm SiC layer, the parameters had to be redetermined for the thicker layer and thus also for the outer pyrocarbon layer. After sintering experiments at 1500°C on already coated particles, which - due to the thicker SiC layer - have a longer residence time in the fluidized bed, no interaction between the kernel material and buffer zone was observed.

It became apparent that the inner PyC layer of the particles with a thicker SiC layer (EUO 2309) displayed an increased anisotropy value. The reason for this may be regarded as the longer residence time at 1500°C during the SiC coating process causing sintering of the inner PyC layer and influencing or increasing the anisotropy factor.

The data for particles with a 36 or 51 µm thick SiC layer are compiled in Table 1. Fig. 6 shows sections through unirradiated particles of both types.

Experiment	**HFR-P4, Caps. 1+3**	**HFR-P4, Capsule 2**
	SL-P1	
Particle batch	**EUO 2308**	**EUO 2309**
Kernel		
Composition	UO2	UO2
Stoichiometry U/O	2.006	2.006
Diameter (µm)	497	497
Density (g/cm³)	10.8	10.8
Layer thickness (µm)		
Buffer	94	93
Inner carbon	41	37
SiC	**36**	**51**
Outer pyrocarbon	40	38
Layer density (g/cm³)		
Buffer	1.00	1.00
Inner carbon	1.86	1.86
SiC	3.20	3.20
Outer pyrocarbon	1.88	1.87

Table 1: Particle data

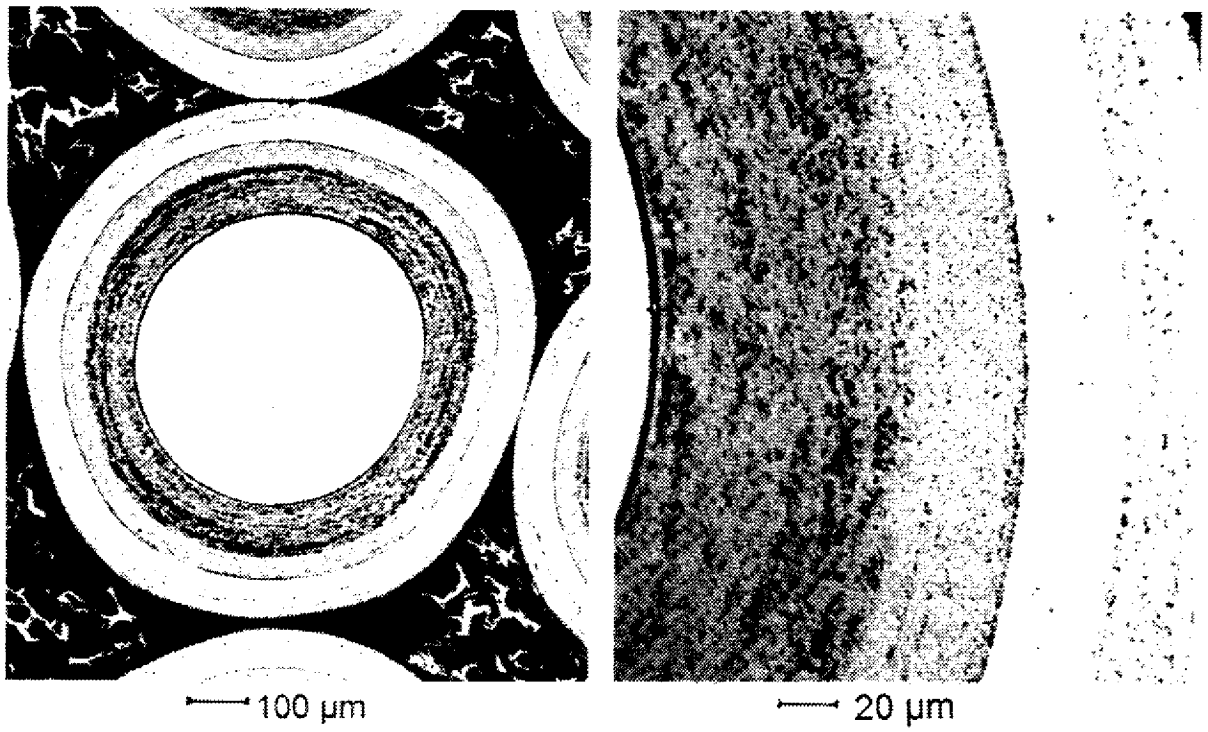

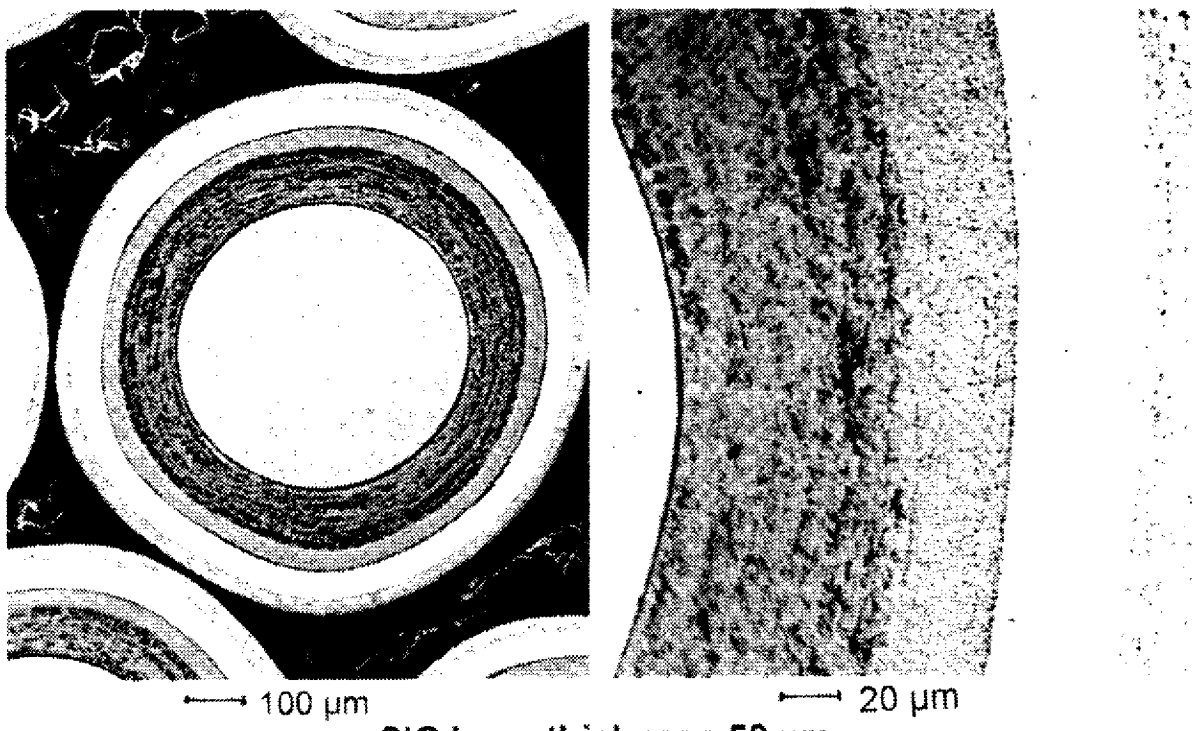

Fig. 6: Cross-section through unirradiated LEU particles with 36 µm (EO 2309), and 51 µm SiC layer

3.3 Compact fabrication

Spherical fuel elements with a reduced fuel zone of 20 mm diameter and a fuel-free zone of 20 mm thickness were moulded according to the conventional procedure at HOBEG resulting in fuel elements with a diameter of 60 mm /21/. A3-27 was used as the matrix graphite. The characteristic data of this matrix type are compiled in Table 2.

		Parallel*	Vertical*
Density	$Mg\ m^{-3}$	1.75	
Thermal conductivity at room temperature	$Wm^{-1}k^{-1}$	75	71
Thermal conductivity at 1000°C	$Wm^{-1}k^{-1}$	35	34
Thermal expansion 20-500°C	$\mu m\ m^{-1}K^{-1}$	2.12	2.38
Anisotropy factor		1.13	
Thermal expansion 20-1000°C	$\mu m\ m^{-1}K^{-1}$	2.67	2.91
Anisotropy factor		1.09	

* to the preferred grain orientation

Table 2: Characteristic data of A3-27 matrix graphite

The fabricated fuel elements were subjected to high-temperature annealing at 1950°C for 1 hour.

Cylindrical compacts were formed from the spherical fuel elements, with diameters of between 23 and 29 mm depending on their vertical position in the capsule in order to achieve a uniform temperature distribution at the surface by means of different gas gaps. In all cases, the height of the compacts was 32 mm. Holes 2 mm in diameter were drilled in the fuel-free zone to accommodate the thermocouples and in the case of the lower compacts, for the gas feed tubes. Three milled spacers on the surface of some compacts ensured centering of the compact column.

During matrix extrusion, X-ray photographs were utilized to ensure that the fuel zone was situated in the centre of the compact and that no particles were destroyed by drilling (Fig. 7).

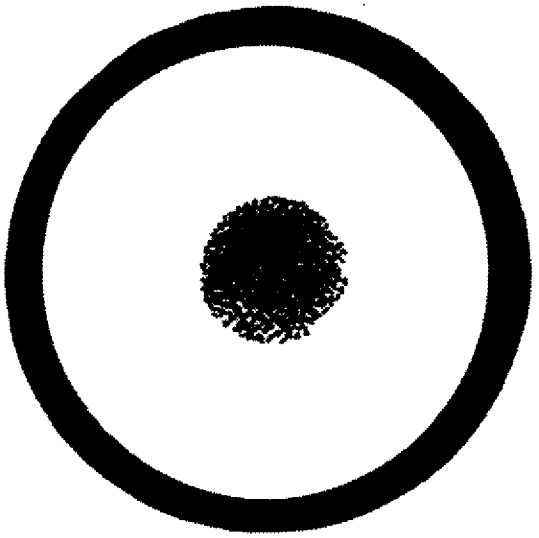

Moulded sphere
(X-ray photograph)

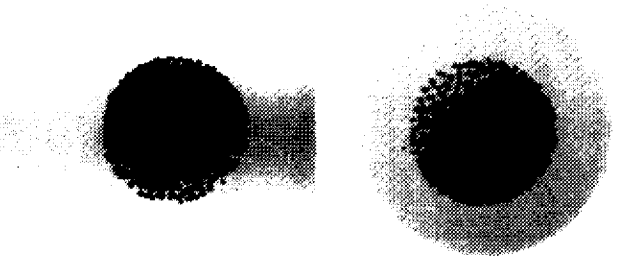

Elevation *Plan view*

After first machining
(X-ray photograph)

Complete compact
(photograph)

Compacts in HFR-P4 capsule (bottom)
(X-ray photograph)

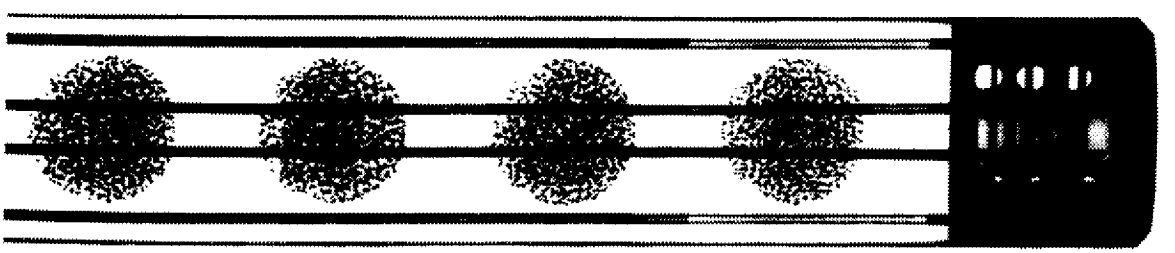

Fig. 7: **Fuel specimens for Experiments HFR-P4 and SL-P1**

The loading data for the compacts of both experiments are compiled in Tab. 3.

Experiment *Particle type* *Matrix*	**HFR-P4** **UO2 TRISO** **NUKEM A3-27**	**SL-P1** **UO2 TRISO** **NUKEM A3-27**
Loading		
U 235 (g/compact)	0.10016	0.10025
Heavy metal (g/compact)	1.018	1.018
U 235 enrichment (%)	9.82	9.82
Number of particles per compact	1631	1666
Particle loading (%)	14.6	12
Dimensions of compacts		
Weight (g/compact)	22.7-32.9	not measured
Diameter (mm)	23-29	30.1
Length (mm)	32	30.8
Diameter of fuel zone (mm)	20	20

Table 3: Loading and Dimensional Data for Compacts in Tests HFR-P4 and SL-P1

4. Irradiation

4.1 Irradiation devices

The irradiation experiment HFR-P4 was irradiated in a TRIO rig at Petten /23/, whereas a TUMULT-G rig at Grenoble was used for the SL-P1 experiment /24, 25/. Diagrammatic representations of the irradiation inserts with the compact numbering system are shown in Fig. 8.

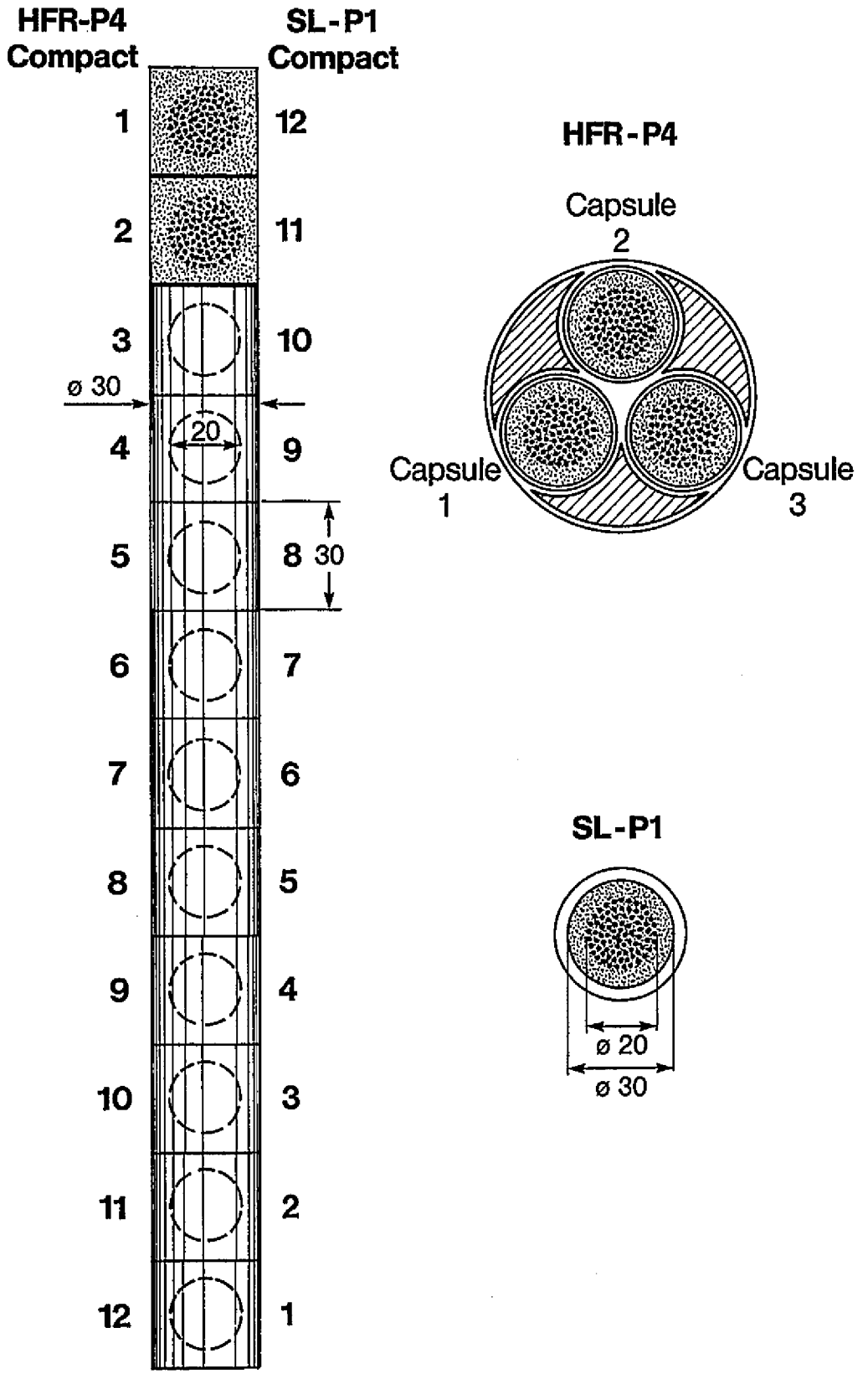

Fig. 8: **Schematic view of irradiation rigs HFR-P4 and SL-P1 (Bold numbers are position designations, two digit numbers are dimensions in mm)**

4.1.1 HFR-P4 irradiation insert

The in-pile section of the HFR-P4 rig consists of three swept and instrumented sample carriers adjacent to each other capable of accommodating 12 compacts each. The irradiation samples are placed in a steel capsule and secured on both sides by graphite discs. Heat shields at either end are intended to reduce the axial heat flux. The constant axial temperature distribution among the samples is achieved by graduated gas gaps between the specimens and containers. Twelve Cr/Al thermocouples with an outer diameter of 1 mm per sample carrier are arranged in six different positions in the fuel-free zone in order to monitor the temperature and two thermocouples are situated in one plane on the opposite sides. The Cr/Al thermocouples in the specimen holder of capsule 3 have a niobium casing.

The temperature is controlled by altering the helium-neon ratio in the purge gas and also by vertically moving the sample carriers in the TRIO capsule. This moving mechanism is also used to maintain the original axial temperature distribution during reactor operation if the flux profile is shifted due to the influence of the control rods.

Flux monitors of niobium foil, Ti and Ni/Co (1 % Co) are incorporated into each sample carrier between the graphite discs at either end and in the centre of the capsules. They are packaged in Al_2O_3 tubes with an external diameter of 1.5 mm and a length of 20 mm. One fission neutron detector is located in the in-pile section of the TRIO capsule in specimen holder 1 so that the thermal neutron flux density can directly be determined. The reading is correlated to the initial power and the flux calibration and is used during irradiation to determine the burnup and the R/B values. A further fission neutron detector is located in the cooling water channel of the TRIO rig.

The purging and control gas circuits newly installed at the HFR Petten permit continuous monitoring and recording of the entire irradiation process /26/. The gas flow rate, gas pressure, sample temperature, neutron flux and fission gas activity are continuously monitored and the data stored. The observation of the released fission gas isotopes towards the end of irradiation was particularly important for HFR-P4 in order to immediately identify the start of particle failure. If, due to rising R/B values of fission gases, there should be a suspicion that particles with the thinner SiC layer are defective then the test would have to be discontinued.

The sweep-gas circuits are designed for continuous withdrawal, monitoring and recording of the released fission gas isotopes as well as for temperature control of

the irradiation samples. Six capsules can be connected and recorded separately. These installations enable fission gas release rates to be measured up to R/B values of 10^{-2} at a fission power of 10 kW per rig. The flow rate of the purge gas is between 1 and 10 $Ncm^3\ sec^{-1}$ at an operating pressure of 5 bar.

Each fuel sample capsule is equipped with two inlet and one outlet tube for the purge gas. Two gases (helium and neon) flow from the gas supply to the gas mixing station where the percentage of neon in the helium is adjusted by control valves in accordance with the specified sample temperature. (He is better in conducting heat, Ne is used to achieve maximum temperatures.)

The specimen temperature, neutron flux, gas pressure, flow rate, purity of the purge gases and purge gas activity are continuously measured and recorded. Activity monitors continuously monitor the purge gas at various locations and are connected electrically to control circuits. In the case of increased activity, the outflowing gas can be retained in receiving tanks.

The most important value for assessing irradiation behaviour and the integrity of the sample is - as long as the experiment is in the reactor - the ratio between the release rate (R) and formation rate (B) of the fission gas isotopes.

Qualitative and quantitative analyses of the fission gas isotopes are undertaken at a gas analysis station. Purge gas samples to determine the activity values by qualitative gas analyses of short-lived fission gas isotopes are taken continuously throughout the entire irradiation time. Gamma spectrometry measurements of the long-lived fission gas isotopes are performed at daily intervals for quantitative gas analysis.

Various measuring techniques are employed to measure short- and long-lived fission gas isotopes:

- on-line measuring techniques for short-lived isotopes in which the purge gas flows continuously through a measuring tank and is simultaneously measured (^{89}Kr, ^{137}Xe, ^{138}Xe ^{135m}Xe)

- direct volume measurement for longer-lived isotopes, where the purge gas is fed through the measuring tank, then isolated and measured after a certain time (^{138}Xe, ^{135m}Xe).

A standard value for the B values is stored in the data base for on-line determination of the R/B values. After each cycle burnup calculations are performed and the R/B values corrected. A precise description of the instrumentation and gas analysis is given in /26/.

All relevant data of the irradiation experiment, instrumentation information, data storage and calculations of the reactor-specific characteristics for implementing the experiment as well as the work planned by Petten are described in detail in the safety Report by the HFR Division /23/.

4.1.2 SL-P1 activation test

In order to establish the fabrication-induced particle defects before being irradiated in SILOE, an activation test was performed in the MELUSINE reactor in which the fission gas release from the 12 compacts was measured in a low neutron flux /27/.

In the selected irradiation position the MELUSINE reactor power was 8 MW, the calculated thermal flux 0.8 x 10^{16} $m^{-2}s^{-1}$ and the gamma power in the graphite 0.2 W/g. The temperatures were in the range from 660 to 680°C. The individual irradiations lasted a maximum of 30 minutes and during this time it was possible to perform two fission gas withdrawals per capsule.

In this case, loose particles of the EUO 2308 type as also used in the compacts were available for dosimetry. Four particles each were irradiated in small graphite containers as dosimeters and subsequently evaluated by gamma spectrometry.

In most cases, release of fission gases from the compacts was below the detection limit. An estimate indicated that the R/B values of the released Kr-isotopes must be less than 10^{-8}. It was thus possible to demonstrate that no fabrication-induced particle defects or increased contamination was present /27/.

4.1.3 Irradiation insert SL-P1

A modified TUMULT-G rig was used in the irradiation test. The capsule was swept by He and temperatures were measured and controlled. The rig was designed in such a way that a fuel temperature of 800°C was achieved. 14 Cr/Al thermocouples were inserted into the fuel-free zone of the compact for temperature monitoring.

The rig is swept with two independent gas circuits. One circuit flows through the inside of the capsule and sweeps the compacts with pure helium. This circuit is used both to flush out impurities and also to withdraw fission gas samples. The other, outer circuit contains a gas mixture of helium and neon and is exclusively used for temperature control.

Three fission neutron monitors at three measuring points were employed (top, centre, bottom) and eight dosimeters (Nb, Cu, Cu/Co) at five measuring points are used for the dosimetry. The tubes containing the monitors are secured in the reactor core.

The irradiation rig is inserted vertically into the reactor in order to achieve the most homogeneous possible temperature profile over the 12 compacts. It is also possible to correct the temperature by raising the rig by 100 mm from the lowest point.
The axial irradiation positions were chosen to compensate for the decrease in fuel power (due to ^{235}U burnup).

4.2. Irradiation target values

Design calculations for LEU cores of future HTR plants formed the basis of planned irradiation data for HFR-P4 and SL-P1. Nominal values expected for the neutron fluence and burnup in future plants are ~2.5×10^{25} m^{-2} (E>16fJ) and 8.9 % FIMA, respectively, for LEU fuel elements (this is about 25 % below the corresponding values for an HEU/Th fuelled HTR). In the tests performed, the failure behaviour of the particles was to be demonstrated for a fuel element meeting expected licensing-basis requirements of neutron fluence and burnup of 5×10^{25} m^{-2} (E>16fJ) and 11 % FIMA, respectively. In order to provide further safety margin, design-basis values of 6.4×10^{25} m^{-2} (E>16fJ) and 13 % FIMA were also specified to explore the performance margins of modern LEU HTR fuel. The HFR-P4 and SL-P1 tests were designed to give fuel performance behaviour up to the above fluence and burnup values. At the same time, it was planned that the experiments should not be terminated after fixed irradiation parameters, but rather after a failure fraction of 0,5 % (5×10^{-3}) had been reached.

The fuel temperatures should remain constant throughout the entire irradiation time. The specified surface temperature is to be achieved at the ends of the capsule by adjusting the gas gaps.

Based on predictive simulations of the irradiation experiment HFR-P4, an irradiation temperature of 1000°C had been recommended for the comparison of particles with 36 µm thick SiC with those of 51 µm. Design temperatures were:

HFR-P4	Capsule 1	Capsule 2	Capsule 3
Design temperature (centre)	1000°C	1000°C	1200°C
SiC layer thickness	36 µm	51 µm	36 µm

Actual irradiation temperatures were eventually well below the design target (see Fig. 9).

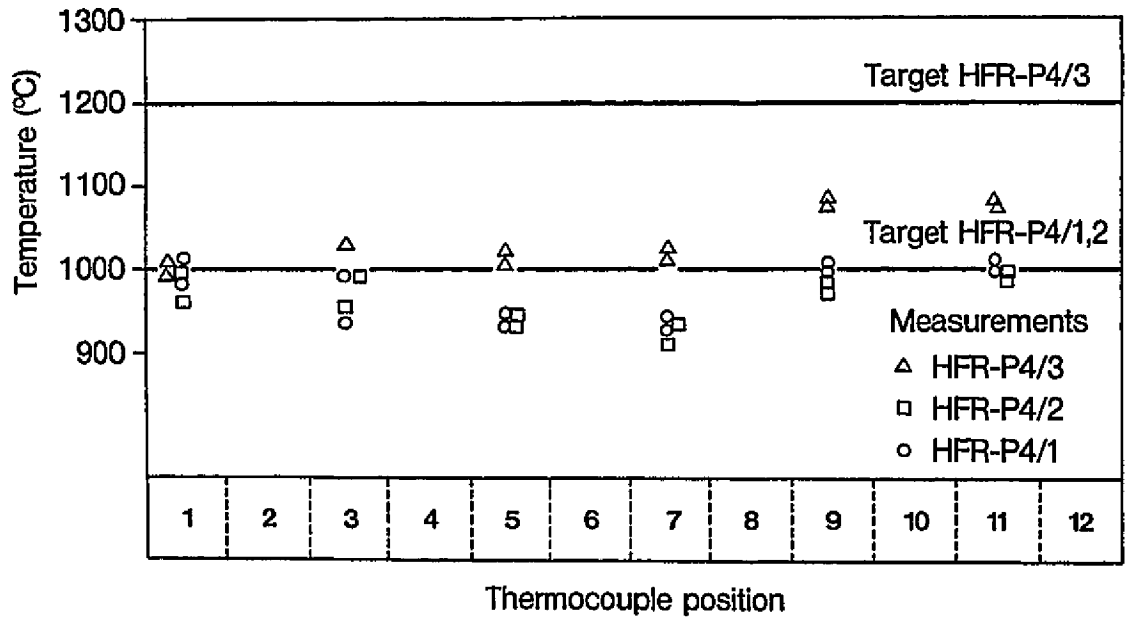

Fig. 9: **Axial temperature distribution in experiment HFR-P4**

4.3 Irradiation results

Both experiments, HFR-P4 and SL-P1, were irradiated for just under one full power year. The most important data are compiled in Tab. 4.

Experiment	HFR-P4			SL-P1	HTR MODUL	
Start	10.06.82			24.06.82		
End	28.11.83			23.12.83		
Duration (efpd)	351			330		
Capsule	1	2	3		Expected	Design
Max. burnup (%FIMA)	14.7	14.9	14.0	11,3	8,9	9,8
Max. fast fluence (1E+25 1/m², E>16fJ)	8.0	8.0	8.0	6,8	2,1	2,4
Max. temperature (°C)	940	945	1075	790	837	926
Max. power (mW/c.p.)	410				130	150
R/B Kr 85m (BOL)	3.5 E-09		3.6 E-09	5.8 E-07		
R/B Kr 85m (EOL)	8.0 E-08	8.0 E-08	8.0 E-09	1.2 E-06	2 E-07	6 E-07

efdp = effective full power days
BOL = Beginning-Of-Life EOL = End-Of-life

Tab. 4: Irradiation conditions of experiments HFR-P4 and SL-P1 in juxtaposition to HTR MODUL target values

Both HFR-P4 and SL-P1 experiments were irradiated under much more severe conditions by comparison to the expected and design values in a 200 MW thermal HTR-MODUL (except for irradiation times).

4.3.1 HFR-P4 irradiation results

The aim of the HFR-P4 experiment was to determine the fuel performance of two types of particles having different SiC-layer thickness, when irradiated up to very-high fuel burnup and fast-neutron fluence over an "accelerated" reactor time. The effect of a thicker SiC-layer on the retention of solid fission products at 1000°C was to be determined, as was the effect of irradiation temperature on coated particles having the "standard" SiC coating thickness.

The irradiation of Test HFR-P4 was terminated early due to shutdown of the HFR in November 1983 to replace the reactor vessel. The estimated fuel burnups at that time were in the range of 9 - 12 % FIMA, depending on the position of the compact in the capsule. However, measurements of compact burnups in PIE gamma spectrometry were actually significantly higher (as shown in Tables 5 and 7), being in the range of 10 - 15 % FIMA. As a result, the peak fuel burnup exceeded the peak design value of 13 % FIMA.

Relative to the actual temperature distribution in the capsules, errors in the thermal design led to temperature distributions in the capsules that were not constant along the axis; also, the peak design temperature of 1200°C could not be maintained in Capsule 3 (see Figures 9 and 10).

Overall, the experimental fuel performance observed in Test HFR-P4 was excellent. Considering that the actual fuel burnup (up to ~ 15 % FIMA) and fast neutron fluence [up to 8×10^{25} m^{-2} (E>16fJ)] achieved in the test, it becomes apparent that the irradiation behaviour of the particles in the compacts was outstanding. At the end of irradiation, the fission gas release for ^{88}Kr reached only about 10^{-7} in all three capsules meaning that none of the 58,800 coated particles was defective or had been failed during irradiation (Fig. 10).

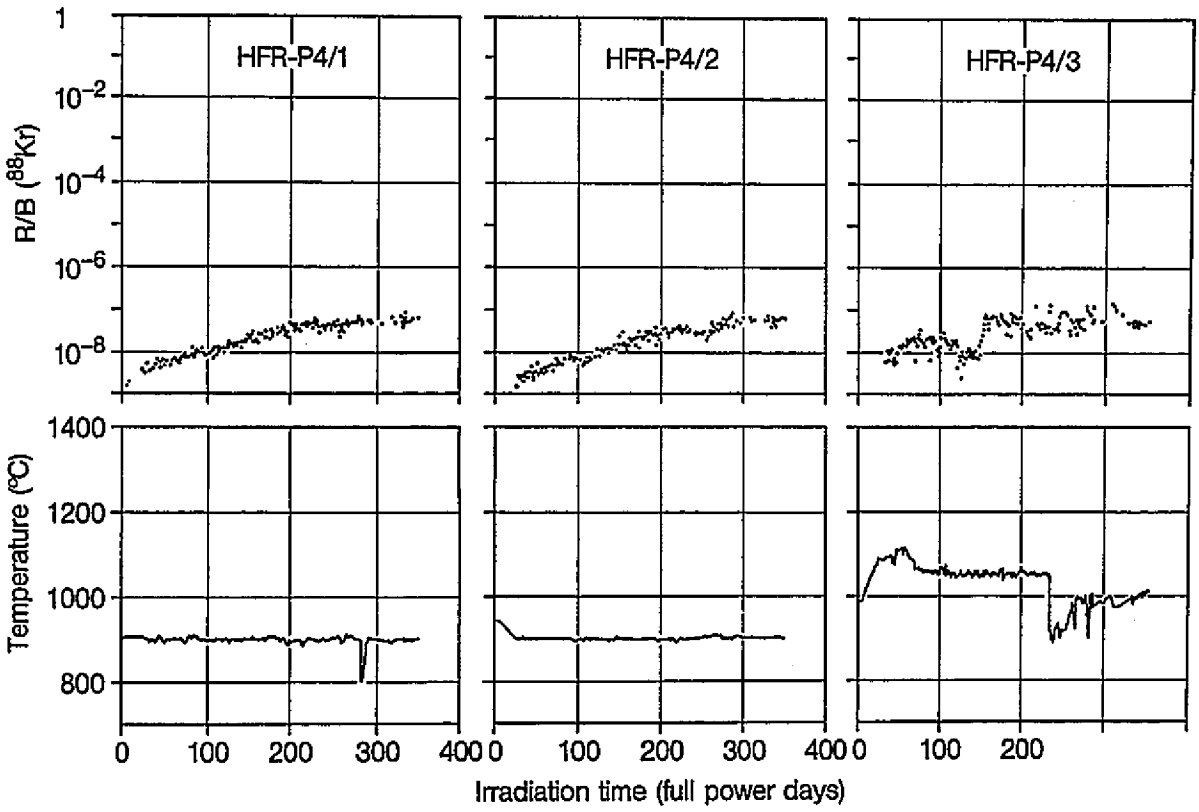

Fig. 10: **Irradiation data of experiment HFR-P4/1/2/3, temperature and R/B values**

HFR-P4 *Compact no.*	*Capsule 1* *Burnup* *(% FIMA)*	*Capsule 2* *Burnup* *(% FIMA)*	*Capsule 3* *Burnup* *(% FIMA)*	*Caps. 1-3* *Fast fluence 1 E+25 1/m² (E>16 fJ)*
1	13.2	13.6	12.5	7.0
2	14.1	14.0	12.9	7.3
3	14.0	14.0	13.3	7.6
4	14.3	14.0	14.7	7.8
5	14.3	14.1	14.0	8.0
6	14.7	14.9	14.0	7.9
7	14.4	14.1	13.9	7.5
8	13.8	13.8	13.1	7.2
9	13.8	12.6	12.6	7.0
10	11.6	12.0	12.5	6.5
11	11.9	11.3	10.9	6.1
12	11.1	9.6	9.9	5.5

Table 5: **Irradiation data from experiment HFR-P4 (KFA values)**

4.3.2 SL-P1 irradiation values

Irradiation in the Siloe reactor started in June 1982 and was terminated in December 1983 after 330 full power days. The aim of the experiment, namely to continue irradiation until particle failure occurred, was not achieved.

As in the HFR-P4 experiment, the compact burnups calculated from irradiation data were underestimated. The evaluation of measurements by gamma spectrometry at the KFA led to considerably higher burnup values (Tab. 6). After 100 irradiation days, the measurements of fission gas release were two orders of magnitude above those in the HFR-P4 capsules, which pointed to a defective particle (Fig. 11). During the activation test in the MELUSINE reactor, the low fission gas release showed that there were no defective particles in the 12 compacts. However, from circumstantial evidence, we must conclude that the MELUSINE test was not reliable.

SL-P1 Compact No.	*Burnup (% FIMA)* KFA	*Burnup (% FIMA)* CENG	*Fast fluence 1E+25 1/m²* *(E>16 fJ)*	*Mean matrix temperature (°C)*
lower				
1	**8.63**	6.32	5.0	743
2	**9.19**	7.53	5.4	750
3	**10.01**	8.25	5.8	759
4	**10.63**	7.96	6.2	785
5	**10.88**	8.08	6.5	788
6	**10.69**	8.59	6.7	790
7	**11.26**	9.39	6.8	793
8	**11.07**	9.87	6.6	794
9	**10.69**	8.54	6.3	794
10	**10.32**	8.82	6.0	794
11	**10.38**	9.08	5.7	780
12	**9.51**	8.36	5.2	763
upper				

Tab. 6: Detailed irradiation data experiment SL-P1

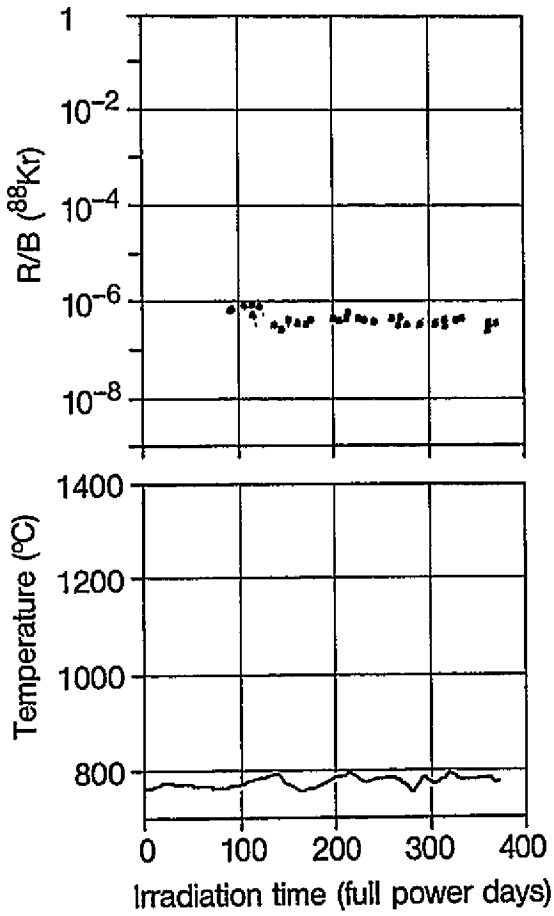

Fig. 11: Gas release and irradiation temperature of experiment SL-P1

5. Post-irradiation examination

The LEU qualification programme comprises the irradiation of six coordinated experiments with low-enriched fuel. A framework for the post-irradiation examination of all LEU experiments was set up in order to maintain a general overview of the post-irradiation examinations and to optimally utilize the existing possibilities.

The main task of all post-irradiation examinations is to demonstrate that the specified target for irradiation-induced particle failure of 2×10^{-4} can be safely met under the test boundary conditions. Further target values are the determination of the particle damage functions, i.e. the dependence of particle failure on temperature, neutron fluence and burnup, the determination of release data for solid (Ag, Cs, Sr) and gaseous (Kr, Xe) fission products from intact and defective LEU-TRISO particles, and the examination of accident behaviour (Chap. 6).

Directly after shutdown, all three capsules in HFR-P4 continued to be swept by pure helium at 50°C. The released krypton was measured in a cold trap to determine the iodine release. Neutron radiography was used to demonstrate that the containers

and specimens had remained intact throughout the 351 day irradiation. Gamma scans along the irradiation tube were performed for several isotopes to determine the axial flux profiles.

5.1 Disassembly, dimension measurements and cold gas test

The capsules from experiment HFR-P4 were dismantled in the Hot Cells at the KFA. Some compact damage had been caused by the thermocouples and gas inlet tubes, especially on the upper compacts.

After disassembly of the irradiation capsule SL-P1 and withdrawal of the compact stack interconnected by the thermocouples, none of the compacts showed any mechanical failure.

Compared with the pre-irradiation values, the dimension measurements of the HFR-P4 compacts show shrinkage or buildup of the graphite matrix under irradiation.

With the aid of the distribution of the fast fluence measured at the cladding, a fluence of fast neutrons can be allocated to each sample. All data measured longitudinally and transversely at 1000°C and 1200°C are compiled in Fig. 12. As in the case of the same sample bodies irradiated at Mol (BR2-P25) with mixed oxide particles /28/, the zero passage for the axial shrinkage was also reached or exceeded here. The same explanation as for the previous experiments is valid for the observed anisotropy of the dimension changes: the fabrication method for small fuel zones does not permit any additional blending in the kernel and thus leads to a higher anisotropy of the dimension changes than in the case of spherical fuel elements /28/. The dimension change of the SL-P1 compacts was smaller as a consequence of the lower fluence.

Cold gas tests were performed with all compacts, i.e. the ^{85}Kr release was measured at 60°C /29, 30/. Increased fission gas releases were measured for two HFR-P4 and one SL-P1 compact, pointing to a particle failure (Tables 11 and 12) /30/. These measurements were confirmed by the later hot gas chlorination (Chap. 5.3 and 5.4) on two of the three compacts with increased releases. With the releasing HFR-P4 compacts both in position 1 of low fluence and burnup, this cannot be an irradiation induced effect.

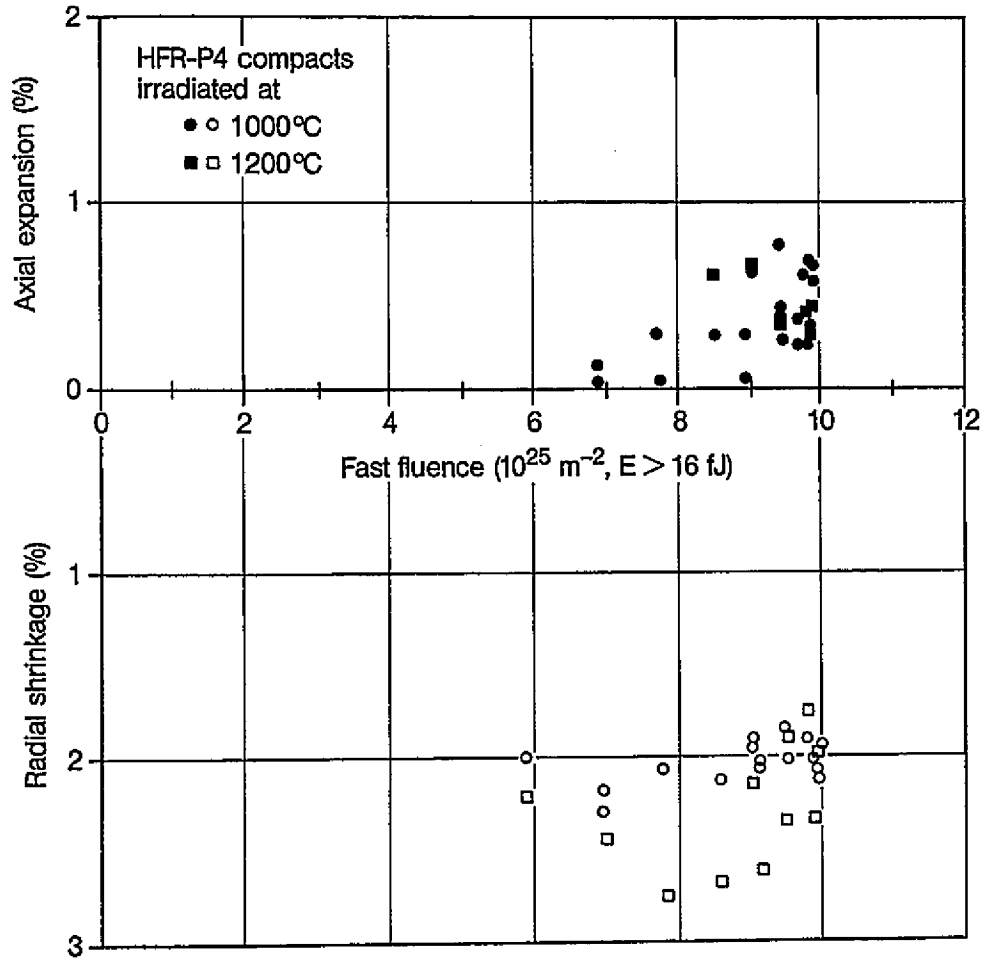

Fig 12: Dimensional changes on compacts in experiment HFR-P4/1/2/3

5.2 Gamma spectrometry for determining the neutron flux, fission product inventory and burnup

Gamma scans of the outer steel tube used during irradiation were first performed on the rotating tube and then at three different angles. The relative activity distributions of the total gamma emission for both ^{54}Mn and ^{60}Co were determined but no other gamma sources were identified. The results were used together with the evaluation by monitors to define exactly the neutron fluence values of each irradiation specimen.

Burnup was determined by the ^{137}Cs inventories. A comparison between the profiles of the fluence of thermal neutrons (determined by gamma scan at Petten) and the burnup values of the HFR-P4 compacts determined by gamma spectrometry is quite satisfactory (Fig. 13).

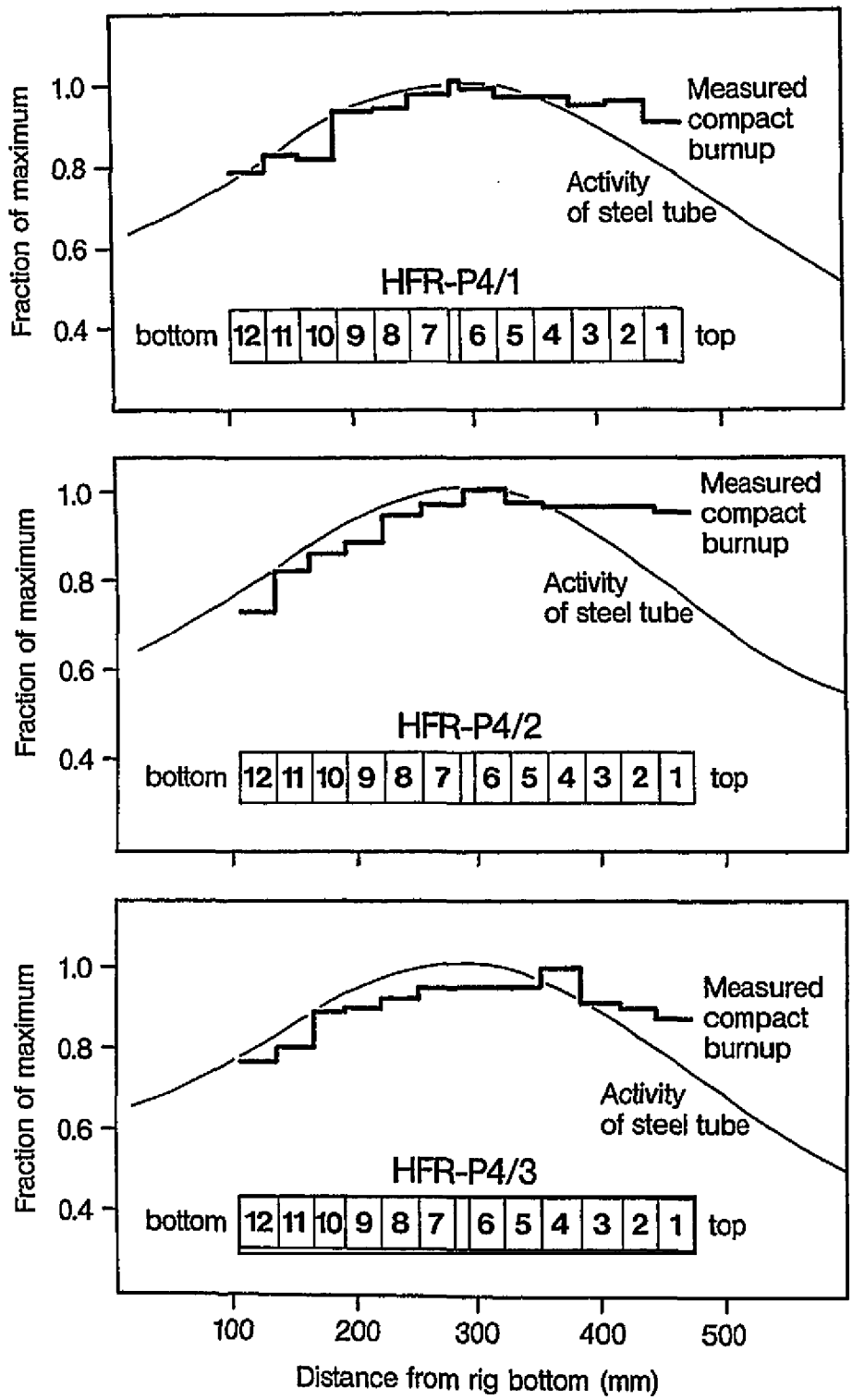

Fig. 13: **Comparison of normalized Cs 137 burnup values with gamma scans on the tubes of experiment HFR-P4**

Both in experiment HFR-P4 and also SL-P1, differences in the burnup values occurred from those determined, on the one hand, from irradiation data at Petten or Grenoble and, on the other hand, from the ^{137}Cs inventories measured at Jülich by gamma spectrometry. The burnups were determined by gamma spectrometry (^{137}Cs) and mass spectrometry (U, Pu) on statistically significant individual particles from two HFR-P4 and one SL-P1 compact at the Research Centre Seibersdorf /31/.

The values obtained with the two methods were in quite good agreement although there were differences from the reactor operators' values - and also from those determined at the Hot Cells (HZ) in Jülich (Tab. 7).

Determination of burnup		***Burnup (% FIMA)***		
Institution	*Method*	*HFR-P4, 1.6*	*HFR-P4, 2.6*	*SL-P1/20*
Reactor	Irradiation data	11.6	11.6	9.4
KFA-HZ	With Cs-137 inventory	14.7	14.9	11.3
OEFZS	With Cs-137/U-235 inventories	13.5	12.6	9.8
OEFZS	Measurement of U/Pu isotopes	13.4	12.4	9.8

Table 7: Comparison of burnup values determined by different institutions with different methods

Although the Seibersdorf burnup values are 4 to 14 % above the reactor data they are 9 to 18 % below the HZ data. For the sake of completeness, the HZ values are used in this report.

The fission power per compact was calculated for each irradiation cycle with the INVENTORY code. The mean fission power per particle in the first irradiation cycle of 23 days together with the ^{137}Cs inventory is shown for the compacts in HFR-P4 capsule 1 in Fig. 14 /32/. At 410 mW per particle the upper limit for the particle power of 300 m W set for the HTR-MODUL was clearly exceeded. The expected value for the particle power in a MODUL is 130 mW per particle.

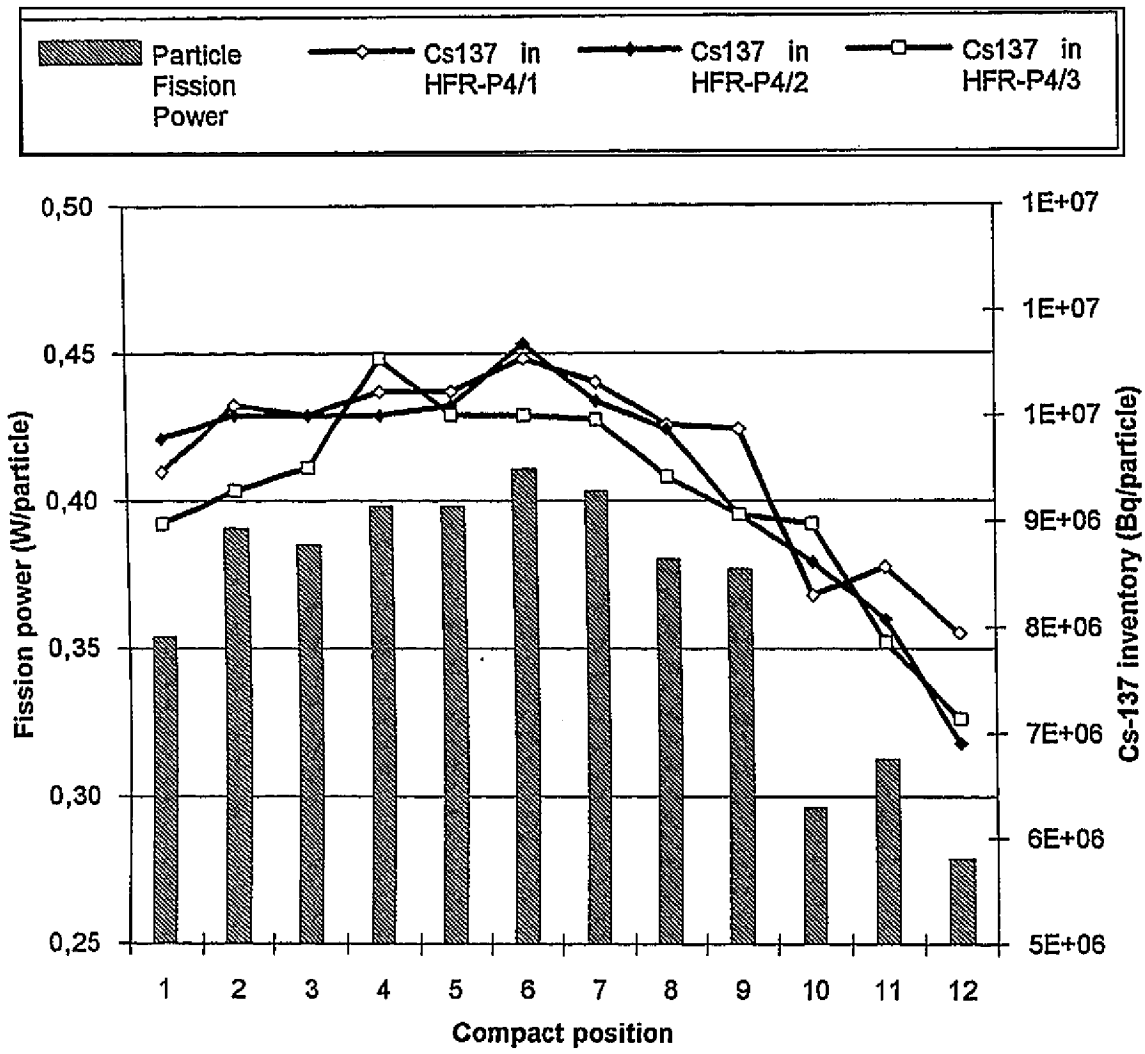

Fig. 14: Particle fission power during first HFR-P4/1 irradiation cycle in comparison to particle ^{137}Cs inventories after end-of-irradiation

The heavy metal inventories were also calculated. The most important values for the start and end of irradiation are compiled in Tab. 8.

Compact	Irradiation time	Burnup (% FIMA)	Heavy metal inventory (g)			
			U-235	U-238	Pu-239	Pu-241
All compacts before irradiation			0.100	0.920		
SL-P1, 7	330 d	11.3	0.006	0.870	0.0116	0.002
HFR-P4, 1.6	315 d	14.7	0.100	0.083	0.0153	0.0028
HFR-P4, 2.6	315 d	14.9	0.002	0.830	0.0152	0.0028
HFR-P4, 3.1	315 d	12.5	0.006	0.850	0.0155	0.0027

Table 8: Calculated heavy metal inventories in SL-P1 and HFR-P4 compacts before and after irradiation

Within the framework of the investigations on burnup determination performed at OEFZS, fission product fractions in the kernel and coating were additionally measured on individual particles after they had been cracked. The results compiled in Tab. 9 show that due to the higher irradiation temperatures the internal release into the coating of the HFR-P4 particles is considerably higher than in the SL-P1 particles. In contrast, cerium does not diffuse at these temperatures and it is only released by recoil from the kernel surface /31/.

Particle from compact	No. of meas. particles	Burnup (% FIMA)	Irradiation temp. (°C)	Internal release (%)		
				Cs-134	Cs-137	Ce-144
SL-P1, 7	4	11.3	790	7.0	6.1	3.1
HFR-P4, 1.6	17	14.7	940	24.6	27.8	2.2
HFR-P4, 2.6	13	14.9	945	31.3	35.1	1.7

Table 9: Internal release from fuel kernels in intact particles during irradiation

5.3 Hot gas chlorination

The method of hot gas chlorination of unirradiated and irradiated graphite fuel elements or fuel samples developed at the Research Centre Seibersdorf allows for the quantitative determination of the quantity of "free" heavy metal present in the matrix. Free heavy metal results from fabrication-related defects or irradiation-induced failure of the coating. A particular advantage of the method is that even very small quantities of free Th, U can be detected.

The individual fuel samples used in the facility, in this case compacts, are heated to a temperature of 900°C or 1000°C according to a predetermined heating programme. In order to remove moisture and oxygen, dry argon gas is used for flushing during this phase. After the desired temperature has been reached, the gas supply to the sample carrier is changed to chlorine gas and flushing is carried out for about 50 hours. The metal chlorides sublimed out of the samples are carried with the gas flow into an adsorption column positioned above and separated there. Hot nitric acid is used to dissolve the deposited chlorides.

The samples are subsequently aliquoted and analysed. The free uranium is quantitatively determined by fluorimetry or by mass spectrometry. Sample aliquots are also measured by gamma spectrometry in supplementary studies.

A total of 24 compacts, 6 each from the three capsules of HFR-P4 and the one capsule of SL-P1, were chlorinated and evaluated at the Research Centre Seibersdorf /33/. The investigations led to the following results:

HFR-P4: No defective particle in any of the 6 compacts from capsule 1.
No defective particle in any of the 6 compacts from capsule 2.
One defective particle in compact HFR-P4/3/1. The other 5 compacts from capsule 3 do not display any defective particles.

SL-P1: One defective particle in compact SL-P1/7. The other five compacts do not display any defective particles.

5.4 Comparison of the particle defects determined by various methods

Due to the low heavy metal contamination of modern fuel elements, fission product release is dominated by the number of defective particles. Determination of the number of defective particles was therefore the central objective of the fission gas release measurements in the reactor and post-irradiation examinations. The results obtained by the various methods are compiled in Tables 10 and 11. In comparing the data, the greatest significance is attached to the in-pile fission gas release values because they provide a complete documentation of fuel particle integrity (Fig. 10 and 11). One single defective particle would lead to a leap in release rates by one to two orders of magnitude, followed by a long-term release increase of half to one order of magnitude. No defective particles were apparently contained in any of the three capsules in experiment HFR-P4 (Fig. 10) or resulted during irradiation.

Experiment / capsule		HFR-P4/1				HFR-P4/3				HFR-P4/2			
SiC thickness (µm)		36				36				51			
Max. irradiation temperature (°C)		940				1075				945			
Analysis method		*R/B in-pile*	*Cold gas test*	*Cs pro-file*	*Chlo-rine test*	*R/B in-pile*	*Cold gas test*	*Cs pro-file*	*Chlo-rine test*	*R/B in-pile*	*Cold gas test*	*Cs pro-file*	*Chlo-rine test*
	1	0	0	-	-	0	1	-	1	0	1	-	-
	2	0	0	0	0	0	0	0	0	0	0	0	0
	3	0	0	-	-	0	0	-	-	0	0	-	-
	4	0	0	0	-	0	0	0	-	0	0	1	0
Compact	5	0	0	-	0	0	0	-	0	0	0	-	-
	6	0	0	0	0	0	0	0	0	0	0	0	0
	7	0	0	-	0	0	0	-	-	0	0	-	0
position	8	0	0	0	-	0	0	0	0	0	0	0	-
	9	0	0	-	-	0	0	-	-	0	0	-	0
	10	0	0	0	0	0	0	0	-	0	0	2	-
	11	0	0	-	0	0	0	-	0	0	0	-	0
	12	0	0	-	-	0	0	-	-	0	0	-	-

Table 10: Number of defective and failed particles determined by different analysis methods on HFR-P4 compacts with 1630 particles each

This is contrasted with the results of the cold gas and chlorine gas test at compact HFR-P4/ 3/1 and the cold gas test on compact HFR-P4/2/1 (Table 10). The defects in these two high burnup particles may possibly have arisen during the rundown of the experiment in the reactor. In contrast, compact SL-P1/7 must already have contained a defective particle at the start of irradiation. The first R/B values for Kr 88 measured after about 100 days are already in the region of 10^{-6} (Fig. 11) whereas a release smaller by two orders of magnitude was determined at the same point in all three HFR-P4 capsules (Fig. 10). This one particle defect is confirmed by the results of the cold gas and chlorine gas test on compact SL-P1, 7 (Table 11).

Experiment / capsule		SL-P1			
SiC thickness (µm)		36			
Max. irradiation temperature (°C)		800			
Analysis method		***R/B in-pile***	***Cold gas test***	***Cs profile***	***Chlorination test***
	1	0	0	-	0
	2	0	0	0	0
	3	0	0	-	-
	4	0	0	1	-
Compact	5	0	0	-	0
	6	0	0	1	-
	7	1	1	-	1
position	8	0	0	1	0
	9	0	0	-	-
	10	0	0	1	-
	11	0	0	-	0
	12	0	0	-	-

Table 11: Number of defective and failed particles determined by different analysis methods on SL-P1 compacts with 1630 particles each

The results of the Cs profile measurements are to be regarded in a different light. In the TRISO particle, caesium is only retained by the SiC intermediate layer whereas high internal releases result from the fuel kernel during irradiation. About 30 % of the ^{137}Cs was released internally in particles from two compacts in the HFR-P4 capsule /31/. If only the SiC layer is damaged during fabrication then the fission gases and the significant iodine continue to be retained in the particle but caesium diffuses out of the particle through the intact pyrocarbon layers. Increased Cs profiles in the matrix graphite of the HFR-P4 compacts 2-4 and 2-10, containing particles with a thick SiC layer, point to one or two particles with defective SiC layers. In contrast, no comparable releases were measured from the particles with normal SiC layer thickness in the HFR-P4 capsules 1 and 3 (Table 10). In four of the five SL-P1 compacts examined, caesium profiles indicated the failure of one particle (Table 11). This is unexpected because irradiation conditions of the SL-P1 particles were considerably lower than in HFR-P4. However, the SL-P1 compacts were already activated before the actual irradiation in order to obtain information about fabrication-induced damage.

In summary, it is concluded that only one particle of a total of 78,400 in the HFR-P4 and SL-P1 experiments became defective, i.e. not gastight, during irradiation. This one particle in the compact was very probably damaged at the end of preactivation in the MELUSINE reactor (see Chap. 4.1.2).

The most important data from all irradiation tests with fuel samples with UO_2-TRISO LEU particles are summarized in Table 12. The fission gas release measurements indicate that in no case did particle fail during irradiation. In individual cases (FRJ2-P27), increased R/B values of Kr 85m at the end of irradiation are, with the exception of SL-P1/7/ the consequence of individual fabrication-induced defects.

Experiment	Specimen per capsule	Particle number	Irrad. time (fpd)	Temperature surf./centre (°C)	Burnup (% FIMA)	Fluence (E>1MeV) 1E+25 1/m²	Rel. at end of irrad. R/B Kr 85m	Rel. at end of irrad. Fract. rel. Cs 137
HFR-P4 /1		19,600	351	915 / 940	1.1 to 14.	5.5 to 8.0	8E-08	5E-06
HFR-P4/2	12 small	19,600	351	920 / 945	9.6 to 14.9	5.5 to 8.0	8E-08	5E-06
HFR-P4/3	spheres	19,600	351	1050 / 1075	9.9 to 14.0	5.5 to 8.0	9E-08	2E-05
SL-P1		19,600	330	780 / 800	8.6 to11.3	5.0 to 6.7	1E-06	5E-06
HFR-K3/1		16,400	359	1020 / 1200	7.5	4.0	2E-07	9E-06
HFR-K3/2		16,400	359	700 / 920	10.0	5.8	1E-07	2E-05
HFR-K3/3		16,400	359	700 / 920	10.6	5.9	1E-07	2E-05
HFR-K3/4		16,400	359	1020 / 1220	9.0	4.9	3E-07	1E-05
FRJ2-K13/1	1 fuel	16,400	396	985 / 1125	7.5	0.2	2E-08	2E-05
FRJ2-K13/2	element	16,400	396	990 / 1150	8.0	0.2	2E-09	2E-05
FRJ2-K13/3		16,400	396	990 / 1150	7.9	0.2	7E-09	6E-06
FRJ2-K13/4		16,400	396	980 / 1120	7.6	0.2	7E-09	6E-06
FRJ2-K15/1		9,600	533	800 / 970	14.1	0.2	1E-06	1E-06
FRJ2-K15/2		9,600	533	980 / 1150	15.3	0.2	5E-09	9E-07
FRJ2-K15/3		9,600	533	800 / 990	14.8	0.1	3E-09	4E-07
FRJ2-P27/1	3	7,340	232	880 to 1080	7.6	1.4	2E-06	2E-05
FRJ2-P27/2	compacts	7,340	232	1220 to 1320	8.0	1.7	1E-05	1E-04
FRJ2-P27/3		7,340	232	1080 to 1130	7.6	1.3	1E-07	1E-05
HFR-K5/1		14,600	359	cycled	6.7	4.0	2E-07	
HFR-K5/2		14,600	359	cycled	8.8	5.8	1E-07	
HFR-K5/3		14,600	359	cycled	9.1	5.9	1E-07	not
HFR-K5/4	1 fuel	14,600	359	cycled	8.7	4.9	3E-07	yet
HFR-K6/1	element	14,600	359	cycled	7.2	4.0	2E-07	measured
HFR-K6/2		14,600	359	cycled	9.3	5.8	1E-07	
HFR-K6/3		14,600	359	cycled	9.7	5.9	1E-07	
HFR-K6/4		14,600	359	cycled	9.2	4.9	3E-07	

Table 12: Parameters and results from irradiation tests with UO2 TRISO particles

6. Accident Simulation Tests

To assess the impact of accidents in an HTR, heating experiments in which the releases of fission products are measured and subsequent investigations were implemented on spherical fuel elements and other fuel samples. These are carried out in the Hot Cells of the KFA Jülich. In these experiments, HTR depressurization accidents with failure of the cooling systems are simulated because maximum temperatures thus result in the core of an HTR and as a consequence the highest fission product releases from spherical fuel elements can be achieved /34, 35, 36, 37/.
From 1977 to 1981, major emphasis was placed on fuel elements with mixed oxide (Th, U) O_2 BISO particles, as used in the THTR 300 at Schmehausen /38, 39/.

Since 1983 fuel elements with TRISO particles envisaged for use in future HTRs have been investigated /40/ with major emphasis on the simulation of the depressurization accident in an HTR-MODUL of 200 MWth. Particular significance is attached to these experiments because of this reactor's safety philosophy according to which the fission products should remain confined in the fuel element in all accidents /41/.

Fuel element temperatures of 1620°C were calculated from the afterheat release for the MODUL core in the hottest region as a consequence of a depressurization accident, including a safety margin of 100°C (Fig. 15).

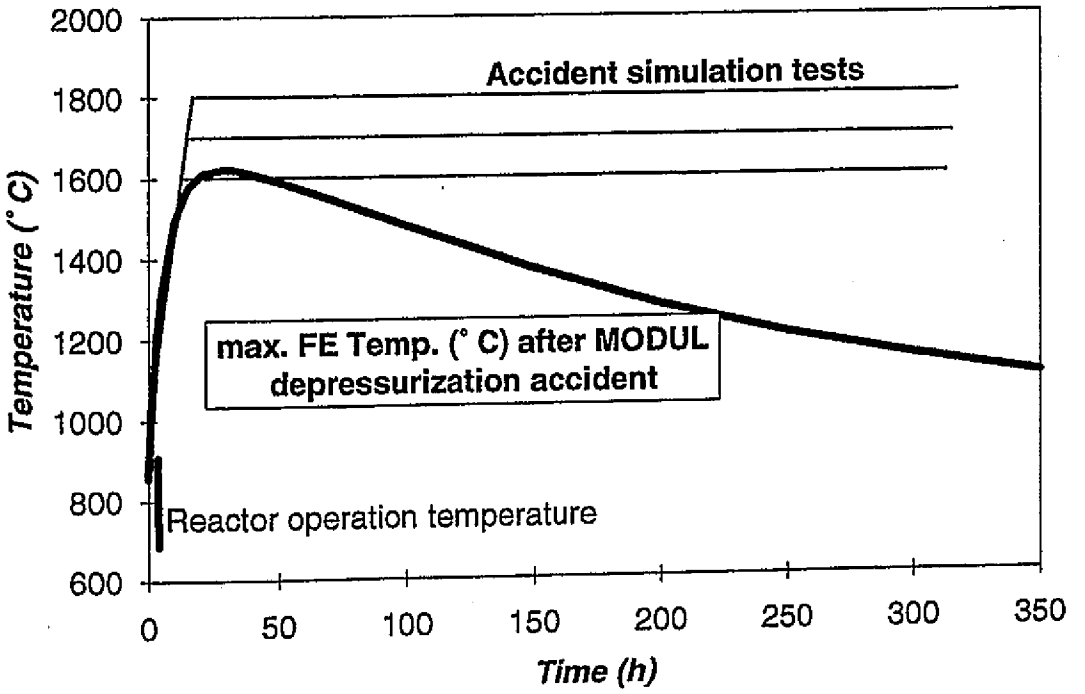

Fig. 15: Temperature evolution during a loss-of-coolant accident in a small HTR and in the heating tests

Fission products	*Half-life*	*Significance*
Solid fission products		
I 131 (I 132)	8 (0.1) days	Of greatest significance for design-basis accidents and licensing
Cs 137 (Cs 134)	30 (2) years	Long-term behaviour after extreme accidents (HTR 500) of significance for risk analyses, Cs 137 more imporant than Sr 90
Sr 90	29 years	
Ag 110m	250 days	Due to the small inventory and limited half-life more important for maintenance than for accidents
Gaseous fission products		
Kr 85	11 years	Unimportant for accident impacts but an indicator of particle defects and iodine release, and easily measurable during heating tests

Table 13: Important fission products in accident simulation with spherical fuel elements and compacts

The accident simulation tests in the 1600 to 1800°C range are intended to investigate the temperature/time conditions under which retention of the important fission products is still maintained. Table 13 gives an overview of these fission products.

6.1 Procedure

The equipment consists of a heating furnace located in a gastight box in the Hot Cell. The furnace is connected to a helium loop working at a slight overpressure with blowers and filters outside the shielded areas (HTRs have a helium pressure of between 1 and 7 MPa during normal operation; the atmospheric pressure in the heating tests is representative of the loss-of-coolant accident). To simulate the slow heatup

characteristics of HTRs and for experimental considerations, the following 30 h procedure (Fig. 16) was established prior to each test: (i) measurement of Kr 85 release at room temperature as a qualitative indication of the state of the fuel; (ii) heating at 300°C for 5 h to clean the helium circuit and remove moisture from graphite components; (iii) simulation of operating temperatures at 1050/1250°C for equilibration of fuel and fission products; (iv) heatup to target temperature at a rate of 47°C/h.

Noble gas traps containing charcoal cooled by liquid nitrogen are located outside the hot cell box. In these gas traps, the activity of ^{85}Kr is monitored by NaI(Tl) detectors which generate the release curves during the heating test. In order to permit measurements of metallic fission products, a water-cooled finger intrudes into the heating furnace and can be removed to replace the condensation plate without interrupting the heating test (Fig. 17). The activity of the plate is measured in a different laboratory with low-level background /14/. In the case of large releases (> 1 % of the sphere inventory), the ^{137}Cs and ^{134}Cs loss can also be determined by comparing gamma spectrometric measurements of the sphere before and after the heating test.

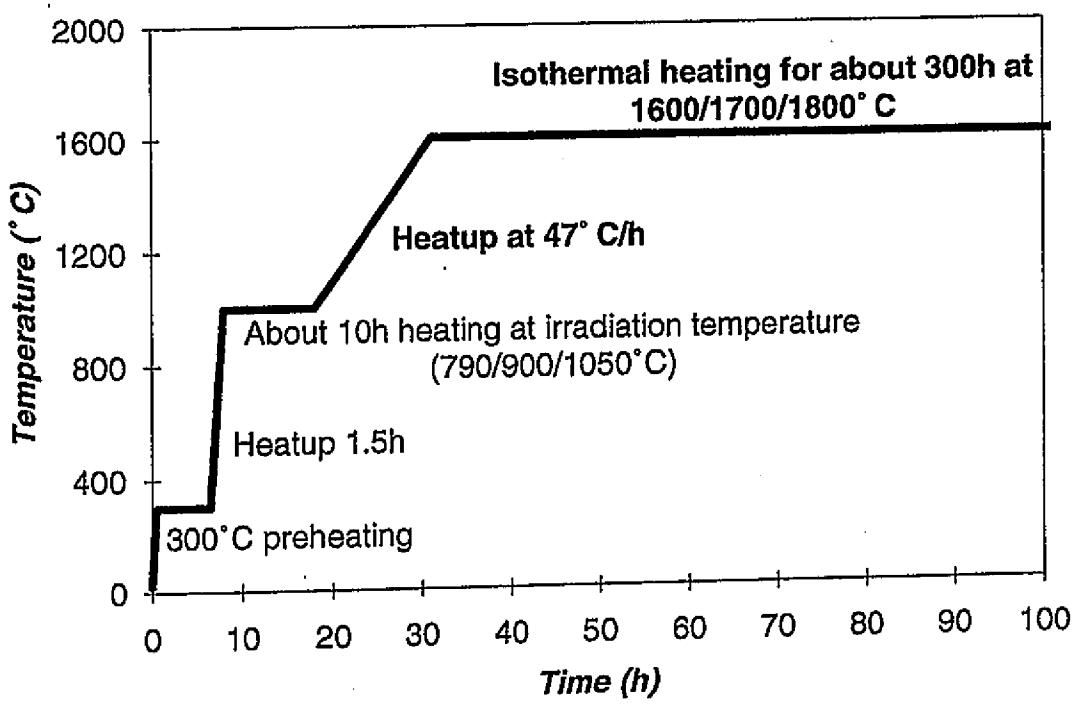

Fig. 16: Details of temperature profile in standardized heating tests

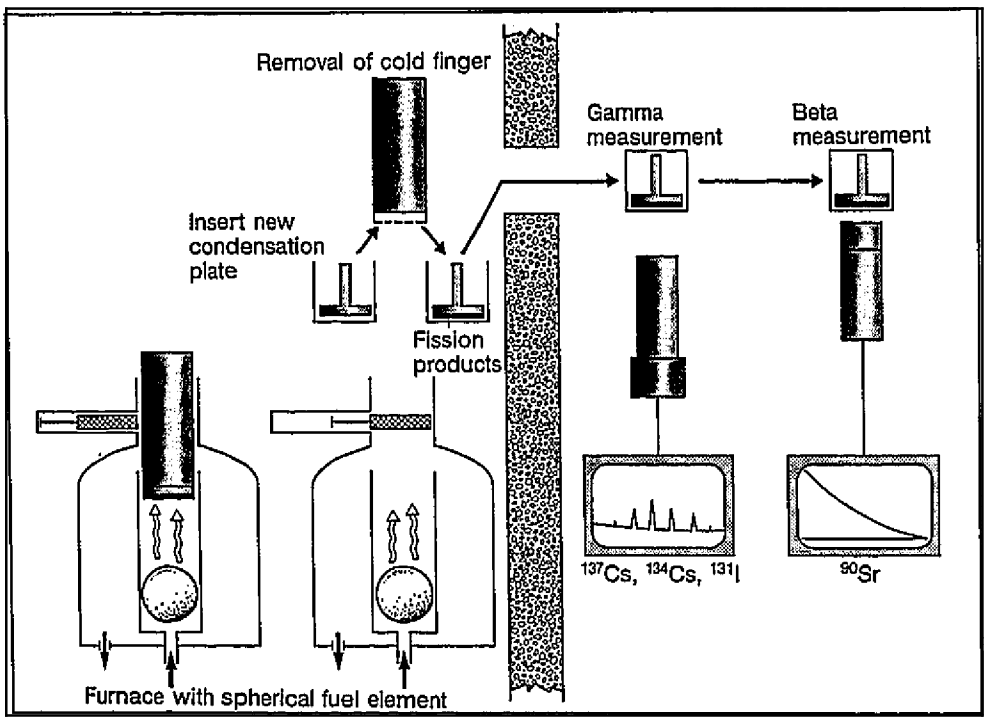

Fig. 17: Schematic diagram of the replacement of the cold finger in the heating furnace and subsequent measurement of deposited activity on the cold finger plate

Further investigations were carried out to obtain additional information about fission product distribution and failures in particle coatings of the heated compacts. The objectives of this work were:

- verification and improved interpretation of release measurements during the heating test,

- data for computer models with which fuel element and core release can be determined /42/.

To this end, the compacts were first electrolytically deconsolidated /40/. The fission product fractions in the matrix graphite were obtained by measuring the graphite and electrolyte samples thus arising. The inventories of individual particles obtained by this deconsolidation were determined by gamma spectrometry, in particular to ascertain the caesium loss. The fission product distribution in the kernel and coating can be determined by cracking individual particles and measuring the kernel and coating fractions /43/.

Furthermore, ceramographic investigations were carried out on particles in order to make changes visible, in particular at the barrier most important for the retention of fission products - the SiC layer.

6.2 Sample data

A total of eight compacts, five from the three capsules of the HFR-P4 experiment and three from the single-capsule rig of SL-P1, were investigated under accident conditions (Tab. 14). The major emphasis of the experiments was placed on the 1600°C test in which compacts with different burnup, including one with particles having a thick SiC layer, were heated. The heating time was 300 hours.

In comparison with the environment of spherical fuel elements in an HTR-MODUL, the burnup/fluence values reached by the compacts studied were very high (Fig. 18).

The calculated or measured fission product inventories of the isotopes investigated here are summarized in Tab. 15.

Fuel compact	*SiC layer (µm)*	*Burnup (%FIMA)*	*Fast fluence 1E+25 (1/m²) (E>16 fJ)*	*Irradiation temp. (°C)*	***Heating test***		
					Temp. T (°C)	*1250...T (h)*	*Duration at T (h)*
SL-P1, 6	36	10.7	6.7	790	**1600**	7.5	304
HFR-P4, 1.12	36	11.1	5.5	900	**1600**	7.5	304
HFR-P4, 1.8	36	13.8	7.2	900	**1600**	7.5	304
HFR-P4, 2.8	51	13.8	7.2	900	**1600**	7.5	304
HFR-P4, 3.7	36	13.9	7.5	1050	**1600**	7.5	304
SL-P1, 10	36	10.3	6	790	**1700**	9	304
SL-P1, 9	36	10.7	6.3	790	**1700**	9	304
HFR-P4, 3.12	36	9.9	5.5	1050	**1800**	12	279

Table 14: Heating programme of accident simulation tests with irradiated fuel compacts

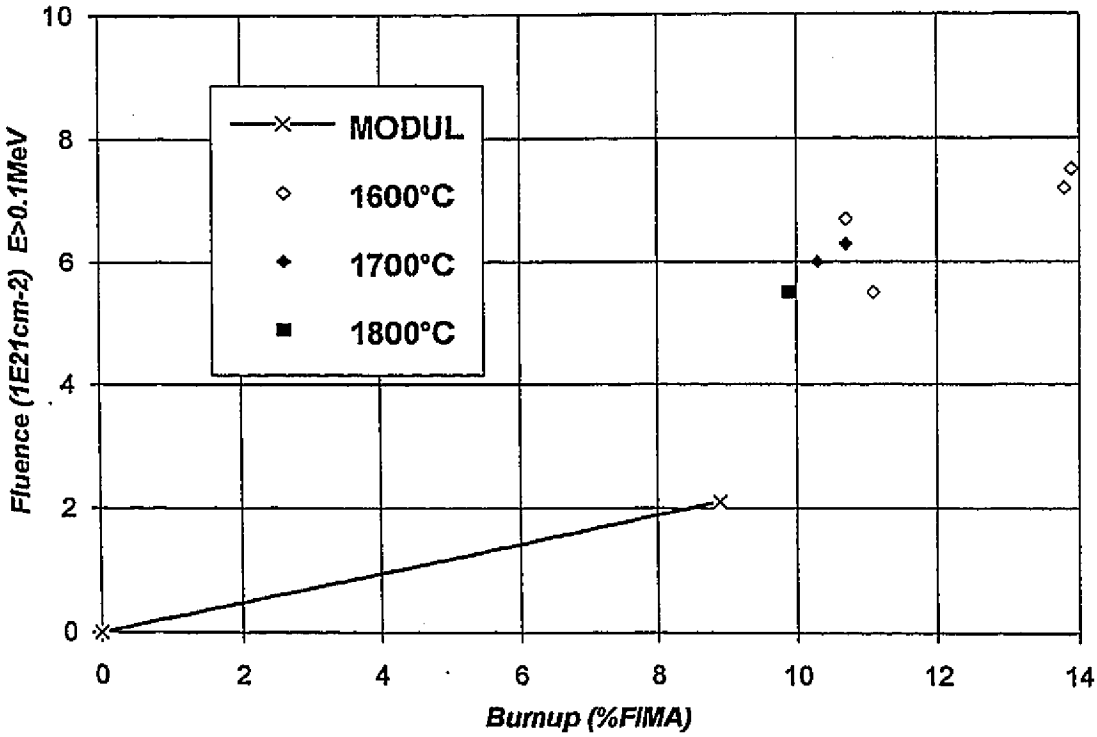

Fig. 18: Irradiation conditions of HFR-P4 and SL-P1 compacts heated at 1600, 1700 and 1800° C compared with conditions in a MODUL HTR

Compact	Burnup (%FIMA)	Inventory (Bq) at end of irradiation					
		Kr 85 Calculated	Sr 90 Calculated	Ag 110m Calculated	Cs 134 Measurem.	Cs 137 Measurem.	Eu 154 Measurem.
SL-P1, 6	10.7	1.17E+09	9.88E+09	3.09E+08	1.91E+10	1.25E+10	6.59E+08
HFR-P4, 1.12	11.1	1.22E+09	9.73E+09	2.48E+08	1.61E+10	1.30E+10	5.26E+08
HFR-P4, 1.8	13.8	1.39E+09	1.11E+10	6.10E+08	2.93E+10	1.62E+10	8.96E+08
HFR-P4, 2.8	13.8	1.39E+09	1.10E+10	5.49E+08	2.78E+10	1.61E+10	8.81E+08
HFR-P4, 3.7	13.9	1.41E+09	1.17E+10	6.17E+08	3.09E+10	1.63E+10	9.45E+08
SL-P1, 10	10.3	1.19E+09	9.20E+09	2.81E+08	1.83E+10	1.25E+10	6.49E+08
SL-P1, 9	10.7	1.17E+09	9.75E+09	2.81E+08	1.83E+10	1.25E+10	6.49E+08
HFR-P4, 3.12	9.9	1.09E+09	7.98E+09	2.07E+08	1.53E+10	1.16E+10	4.70E+08

Table 15: Fission product inventory of compacts used in heating tests

6.3 Release from the compacts at 1600 to 1800° C

The diagrams in this chapter show the total accumulated release fractions of important fission products during the isothermal heating temperature relative to the inventory. The curves therefore start with the release value at the end of the heating period.

Figs. 19 to 22 show the krypton, strontium and caesium release profiles from experiments with four compacts at 1600°C. Particular significance is attached to the ^{85}Kr release curves since they provide information about particle defects and the similarly high iodine release /14/. Whereas the ^{85}Kr release remains low for compacts HFR-P4, 1-12 (Fig. 19) and SL-P1, 6 (not shown) at about 11 % FIMA (see also Tab. 16), it rises from the compacts with high burnup of about 14 % FIMA. However, in the case of pressure vessel failures of particles with this level of high burnup complete fission gas release within 20 hours must be expected at 1600°C. With 1600 particles in one compact, the failure of one particle would lead to a ^{85}Kr release of 6×10^{-4}. However, with the rises in activity shown in Fig. 21 and 22, only about 16 % of a particle's ^{85}Kr inventory fractions were released, whereas 1.6 inventory fractions were released for compact HFR-P4/3/7 in Fig. 20. Only in the case of this compact did a pressure vessel defect occur after 47 hours at 1600°C with the breach of all layers of a particle. Furthermore, damage to the structure of the SiC occurred to different extents in the particles of all three compacts due to the diffusion of fission products into the SiC intermediate layer, probably particularly due to the diffusion of caesium /40/. ^{85}Kr is then either increasingly released due to transport through the PyC layers of many particles or as a consequence of damage to a few PyC layers of individual particles. No difference between compact HFR-P4/1/8 and HFR-P4/2/8 irradiated under identical conditions was identified with respect to the difference in SiC layer thickness (Fig. 21 and 22).

In Fig. 23, the ^{85}Kr release curves of the five compacts are compared with those from six fuel elements with burnups of 3.5 to 9 % FIMA. It is apparent that particle coatings can only become permeable in fuel with extremely high burnup (> 11 % FIMA).

Compact HFR-P4/3/7 showing the highest 1600°C fission product releases in figure 20 had also experienced the highest burnup, neutron fluence and irradiation temperature from all the compacts under investigations (compare table 14)/44/.

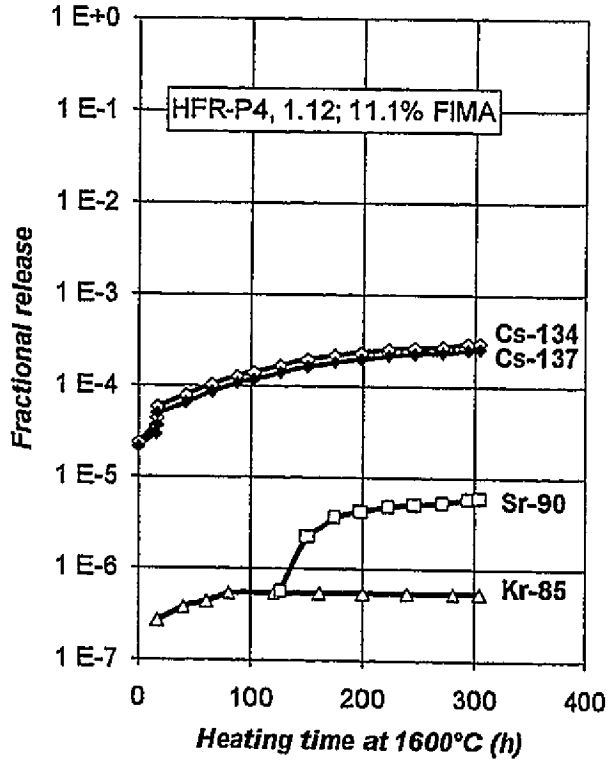

Fig. 19: Release from compact HFR-P4, 1.12 during heating test at 1600° C

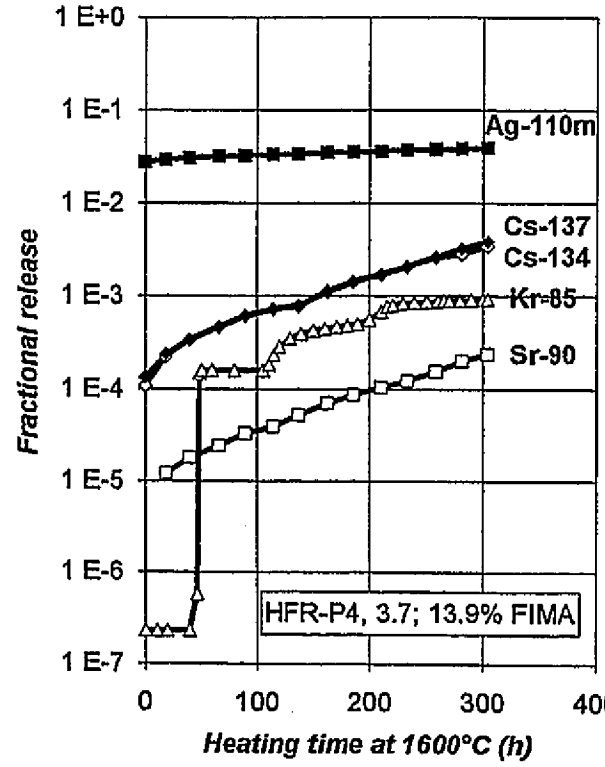

Fig. 20: Release from compact HFR-P4, 3.7 during heating test at 1600° C

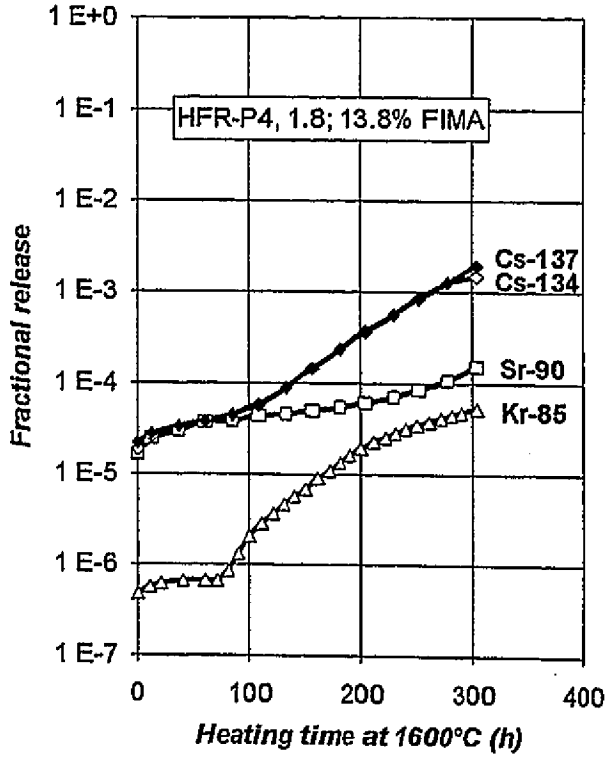

Fig. 21: Release from compact HFR-P4, 1.8 during heating test at 1600° C

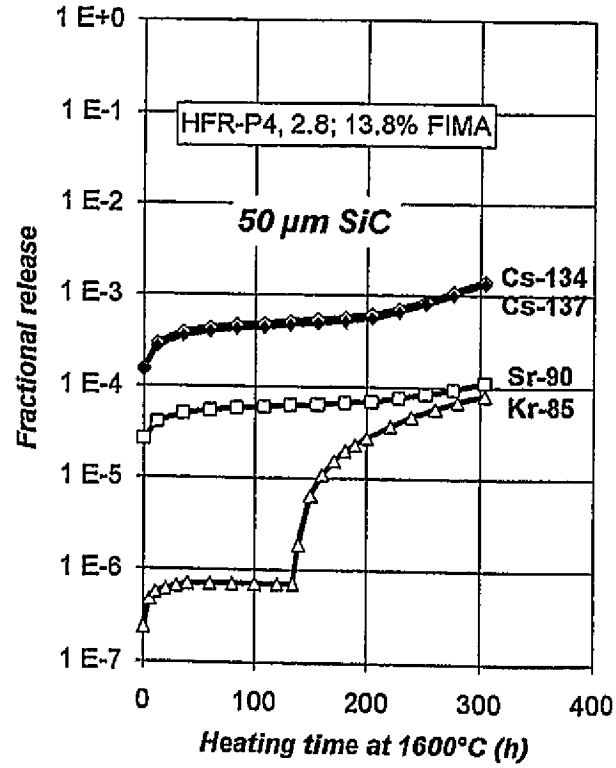

Fig. 22: Release from compact HFR-P4, 2.8 during heating test at 1600° C

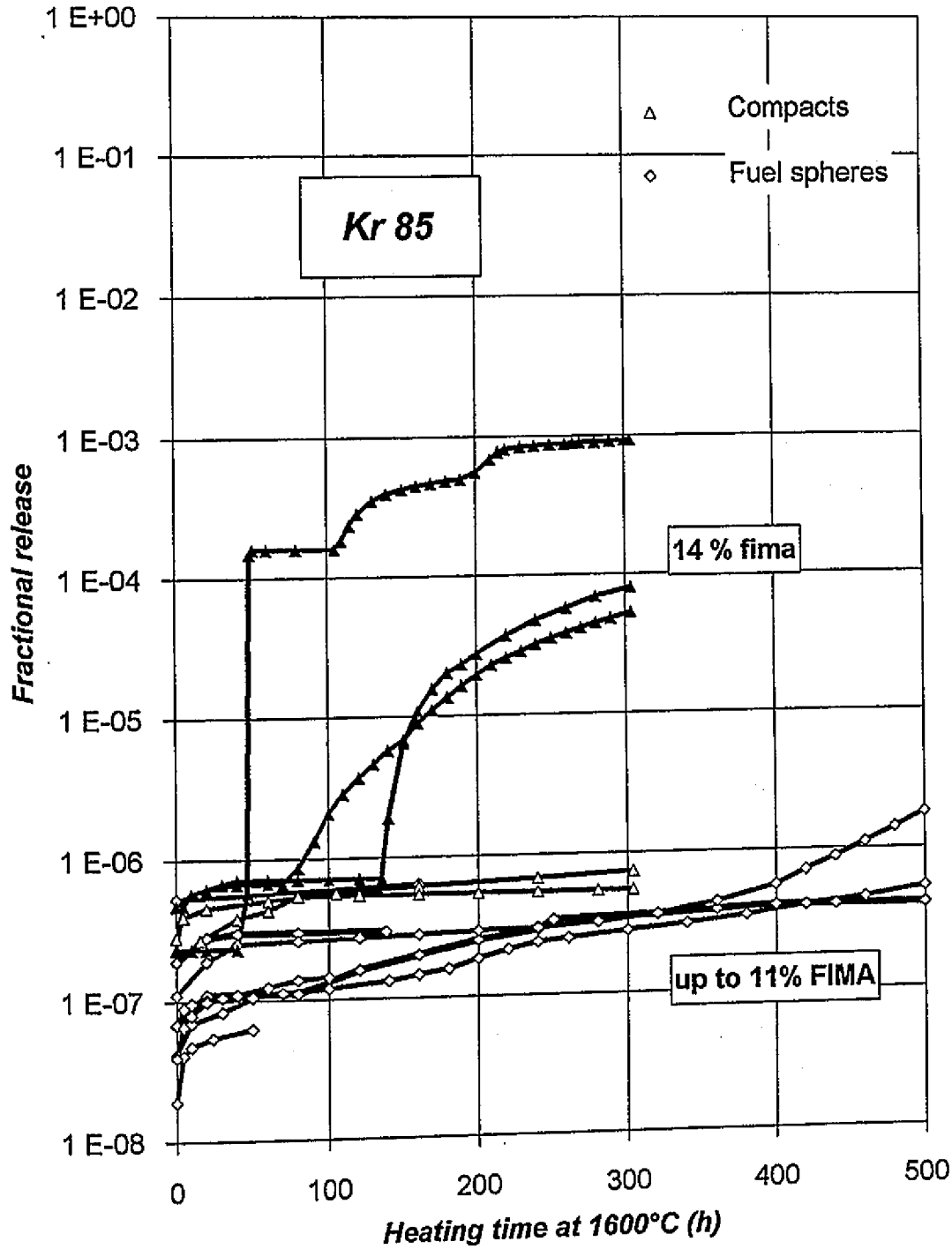

Fig. 23: **^{85}Kr release at 1600° C from compacts (10.7 to 13.9 % FIMA) and fuel spheres (3.5 to 9% FIMA)**

However, two or three particle defects occurred in two out of five AVR spherical fuel elements heated to a maximum of 1620°C according to calculated MODUL accident curves. These fuel elements with burnups of 9.3 % and 9.8 % FIMA respectively had, however, been in operation for 6.5 years in the AVR at on occasion very high temperatures.

Fig. 19 shows the typical sequence of fission product release - as long as no particle defects occur. Caesium release is highest, followed by ^{90}Sr release, which is generally one to two orders of magnitude lower, and the very low ^{85}Kr release in the region of 10^{-7}. Under irradiation conditions as envisaged in the MODUL, caesium is retained in the fuel particles under accident conditions. With the extreme burnup and high irradiation temperature of HFR-P4, together with the long heating time at 1600°C, caesium can be released from intact (= gas retaining) particles, presumably simultaneous with SiC degradation or restructuring, eventually allowing a certain degree of gas release. Figs. 19 and 20 show that the level of caesium release can be correlated with irradiation conditions, which also applies to the strontium release behaviour. The ^{137}Cs releases for all compacts heated at 1600°C and spherical fuel elements with burnups of 3.5 to 9 % FIMA are summarized in Fig. 24. In contrast to ^{85}Kr release, the caesium release increases continuously and is correlated with increasing burnup.

Silver diffuses most rapidly through the particle coating, after longer residence times even starting from 1200°C irradiation temperature. However, due to the low fission yield this is not of such great significance for accident impacts. Since the heating rests only took place three to four years after the end of irradiation, due to its short half-life of 250 days, ^{110m}AG had already decayed to such an extent that it was only measured in compact HFR-P4/3/7 (Fig. 20). Although the fraction of released ^{110m}Ag was one order of magnitude greater than that of caesium at the end of the heating test, its activity was only one third that of caesium.

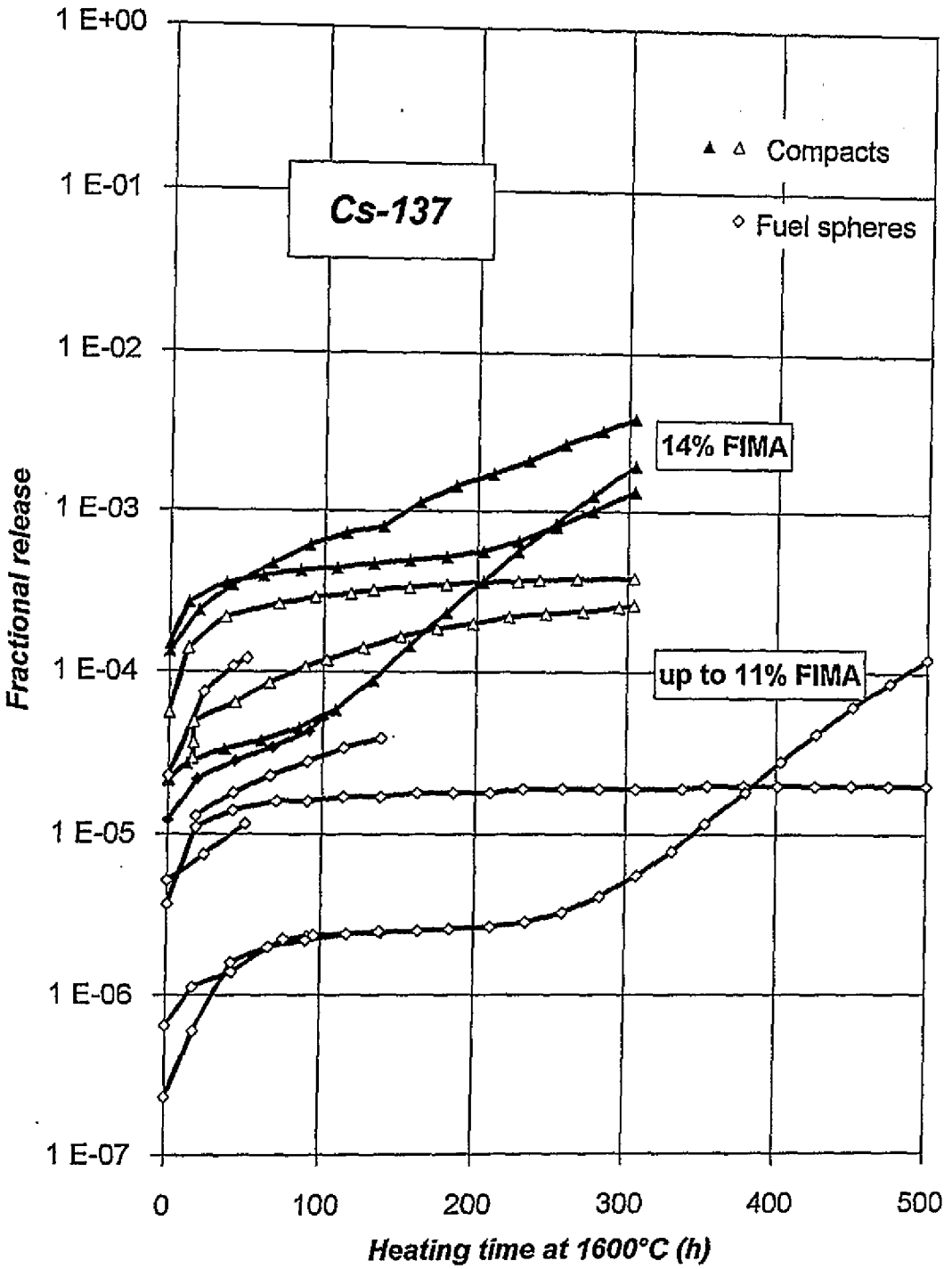

Fig. 24: ^{137}Cs release at 1600° C from compacts (10.7 to 13.9 % FIMA) and fuel spheres (3.5 to 9 % FIMA)

Figs. 25 and 26 show release curves from compacts in heating tests at 1700 and 1800°C. The ^{85}Kr release in Fig. 25 from a compact with 11 % FIMA at 1700°C is similar to those in Fig. 21 and 22 at only 1600°C - but from compacts with a burnup

of 14 % fima. At 1800°C (Fig. 26), the release increases continuously. These are not pressure vessel failure which would lead to a release jump, but coating failures in a large number of particles resulting in an increase in the release of ^{85}Kr after 300 hours to 0.1 % of the inventory.

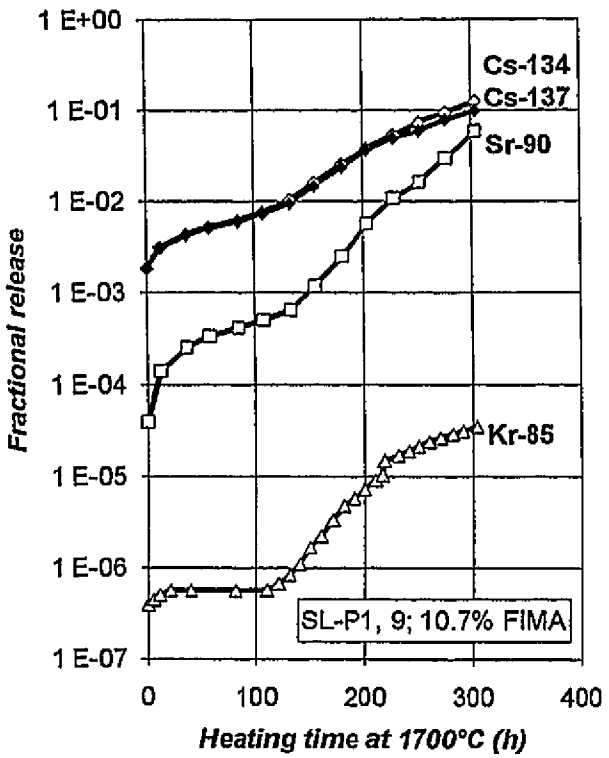

Fig. 25: Release from compact SL-P1, 9 during the heating test at 1700° C

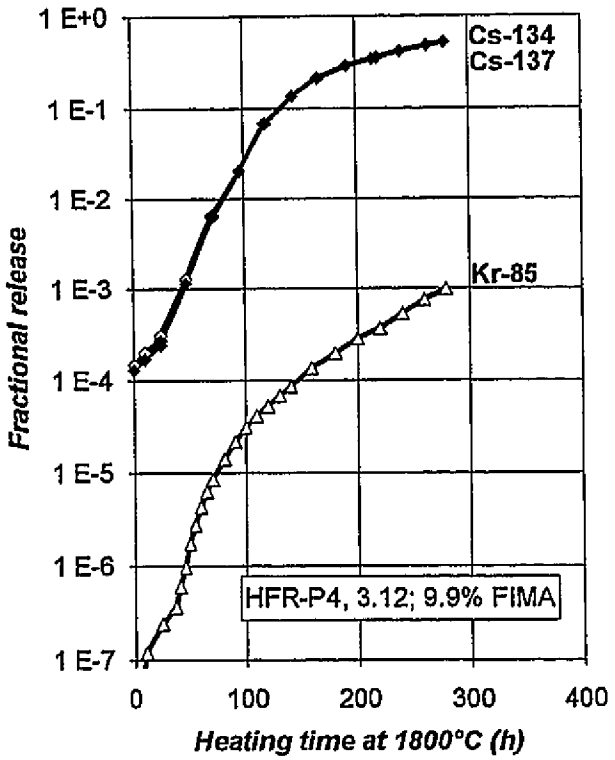

Fig. 26: Release from compact HFR-P4, 3.12 during the heating test at 1800° C

The usual release sequence of caesium/strontium/krypton is also evident clear in Fig. 25. It was not possible to measure the strontium release from compact HFR-P4 3.12 at 1800°C with sufficient accuracy (Fig. 26).

Fig. 27 shows the ^{137}Cs release from compacts with approximately the same burnup at different temperatures. Whereas the Cs retention is still very good at 1600°C in the compact, the release rises at 1700°C to high fractions and even more so at 1800°C during the 300 h isothermal heating tests /46/.

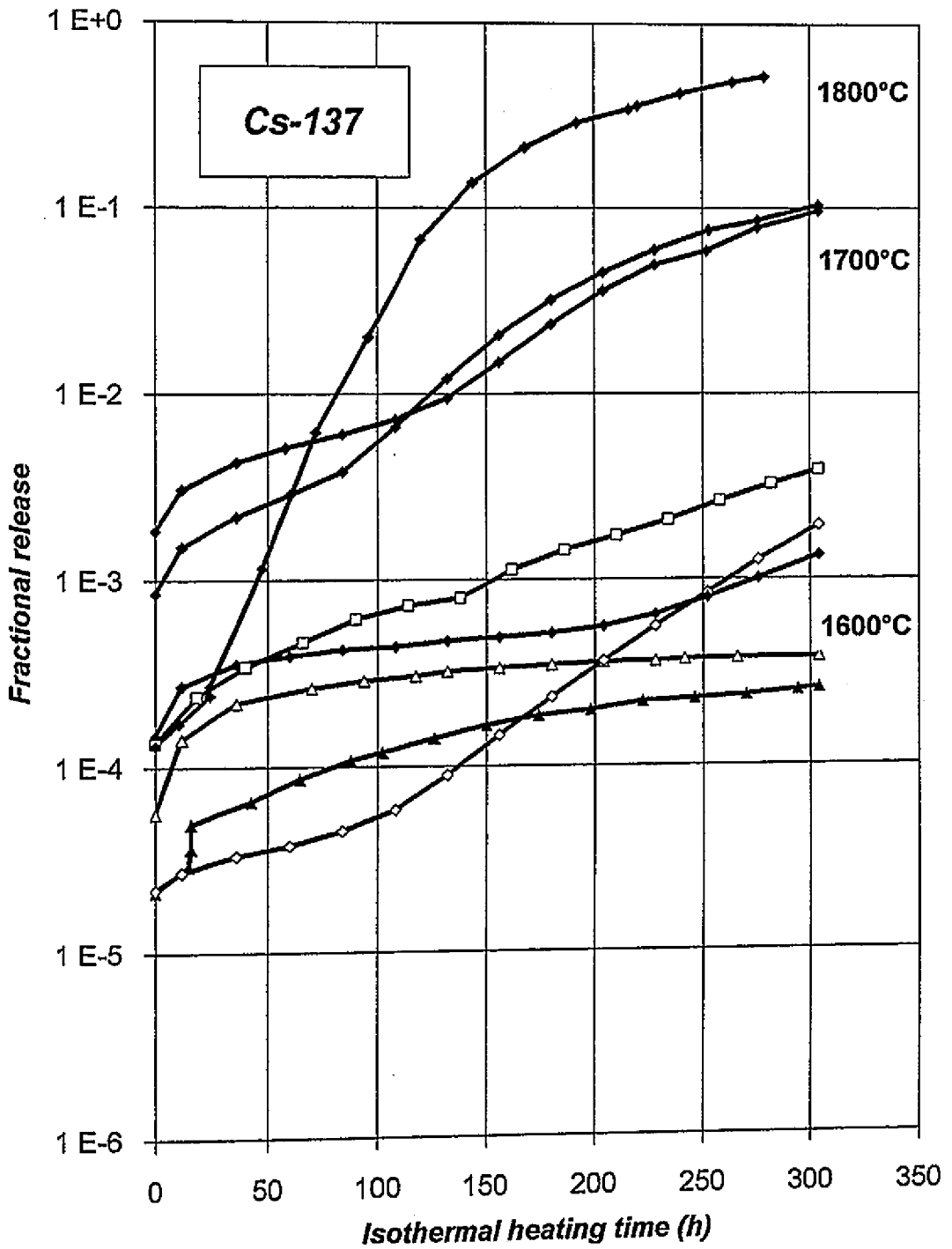

Fig. 27: **^{137}Cs release from compacts with burnup of 10-11% FIMA at 1600, 1700 and 1800° C**

A summary of the overall releases from the accident simulation tests is given in Tab. 16.

Fuel compact	*Burnup*	*Heating*	*Fractional release*					
		temp.	***Kr-85***	***Sr-90***	***Ag-110m***	***Cs-134***	***Cs-137***	***Cs-137***
	(%FIMA)	*(°C)*					*Cond. **	*Inv. ***
SL-P1, 6	10.7	1600	7.33E-07	4.31E-05	Below	7.54E-04	3.88E-04	Below
HFR-P4, 1.12	11.1	1600	5.41E-07	6.00E-06	limit of	3.02E-04	2.60E-04	detection
HFR-P4, 1.8	13.8	1600	5.38E-05	1.53E-04	detection	1.51E-03	1.97E-03	limit
HFR-P4, 2.8	13.8	1600	8.07E-05	1.13E-04		1.45E-03	1.37E-03	1.00E-02
HFR-P4, 3.7	13.9	1600	9.87E-04	2.43E-04	3.90E-04	3.54E-03	3.94E-03	5.00E-03
SL-P1, 10	10.3	1700	9.10E-05	2.06E-02	Below	9.30E-02	1.04E-01	1.10E-01
SL-P1, 9	10.7	1700	3.67E-05	5.83E-02	limit of	1.25E-01	9.75E-02	1.18E-01
HFR-P4, 3.12	9.9	1800	1.01E-03	a)	detection	5.23E-01	5.23E-01	5.60E-01

a) Not measured

* Values from KÜFA condensate plates

** Measurement of compact inventory before and after heating test

Table 16: Results of accident simulation tests with HFR-P4 and SL-P1 compacts

Two values each are given for the ^{137}Cs releases. In the apparatus used it is possible to make measurements even of very low releases by means of a fixed calibrated fraction of the solid fission product deposited on the condensate plates (see Chap. 6.1). The ^{137}Cs loss in the compact can be determined for release fractions greater than 1 %. To this end, the compact to be investigated is measured five times before and after the heating test alternating with a different compact with a similarly high ^{137}Cs inventory. The decrease of the ^{137}Cs inventory during heating can be determined from the ratios of the inventory values in a relatively precise manner, approximately ± 1 % of the inventory. Major errors in determining the caesium release can thus be ruled out by using two completely independent measuring methods.

6.4 Fission product fraction in the matrix graphite

After the heating test the compacts were deconsolidated electrolytically /47/. The electrolyte and graphite samples were measured at the KFA by gamma spectrometry /48/. Aliquots of the samples were, furthermore, also investigated at Harwell and Rossendorf, particularly with respect to ^{90}Sr /49, 50/. The results of the measured nuclides are summarized in Tab. 17. The lowest fraction measured was ^{154}Eu, which was almost completely retained in the fuel kernels even at 1800°C.

UO2-TRISO	*Burnup*	*Fast fluence*	*Irradiation*	*Heating test*		*Fraction in matrix* *			
Compact	*(%FIMA)*	*1E+25 (m-2) E>16 fJ*	*temp. (°C)*	*Temp. (°C)*	*Duration (h)*	*Sr-90*	*Cs-134*	*Cs-137*	*Eu-154*
SL-P1, 6	10.7	6.7	790	1600	304	1.2 E-03	9.4 E-04	9.7 E-04	1.4 E-03
HFR-P4, 1.12	11.1	5.5	900	1600	304	6.7 E-04	6.2 E-04	5.8 E-04	1.2 E-04
HFR-P4, 1.8	13.8	7.2	900	1600	304	2.9 E-03	1.3 E-03	1.3 E-03	2.9 E-04
HFR-P4, 2.8	13.8	7.2	900	1600	304	2.2 E-03	8.1 E-04	8.0 E-04	1.0 E-03
HFR-P4, 3.7	13.9	7.5	1050	1600	304	1.9 E-03	6.3 E-04	1.4 E-03	1.8 E-04
SL-P1, 10	10.3	6	790	1700	304	9.0 E-02	2.4 E-02	2.3 E-02	4.3 E-03
SL-P1, 9	10.7	6.3	790	1700	304	4.5 E-02	3.7 E-02	3.6 E-02	2.2 E-03
HFR-P4, 3.12	9.9	5.5	1050	1800	279	2.3 E-02	5.2 E-02	5.2 E-02	7.6 E-03

* Sr from Rossendorf, Cs and Eu from Jülich measurements

Table 17: Fission product content in matrix graphite of heated compacts

Furthermore, ^{106}Ru, ^{125}Sb and ^{144}Ce were measured in the region of the detection limit. Ruthenium and antimony behave in a similar manner to europium, whereas cerium is regarded as immobile even at 1800°C /40/.

The results of the 90Sr determinations at Harwell and Rossendorf are compared in Fig. 28. The values are in very good agreement. Merely in the case of the SL-P1, 9 graphite value determined at Harwell was an error made either in sampling or measuring.

As expected, the ^{90}Sr fractions are in the matrix low at 1600°C (Fig. 28). This means that even after 300 hours, particularly from the two compacts with lower burnup, SL-P1, 6 and HFR-P4, 1.12, the release from the particles is only about 0.1 %. The

^{90}Sr fraction from compact HFR-P4/2/8 with 51 µm SiC is only slightly lower with the normal SiC layer than HFR-P4/1/8.

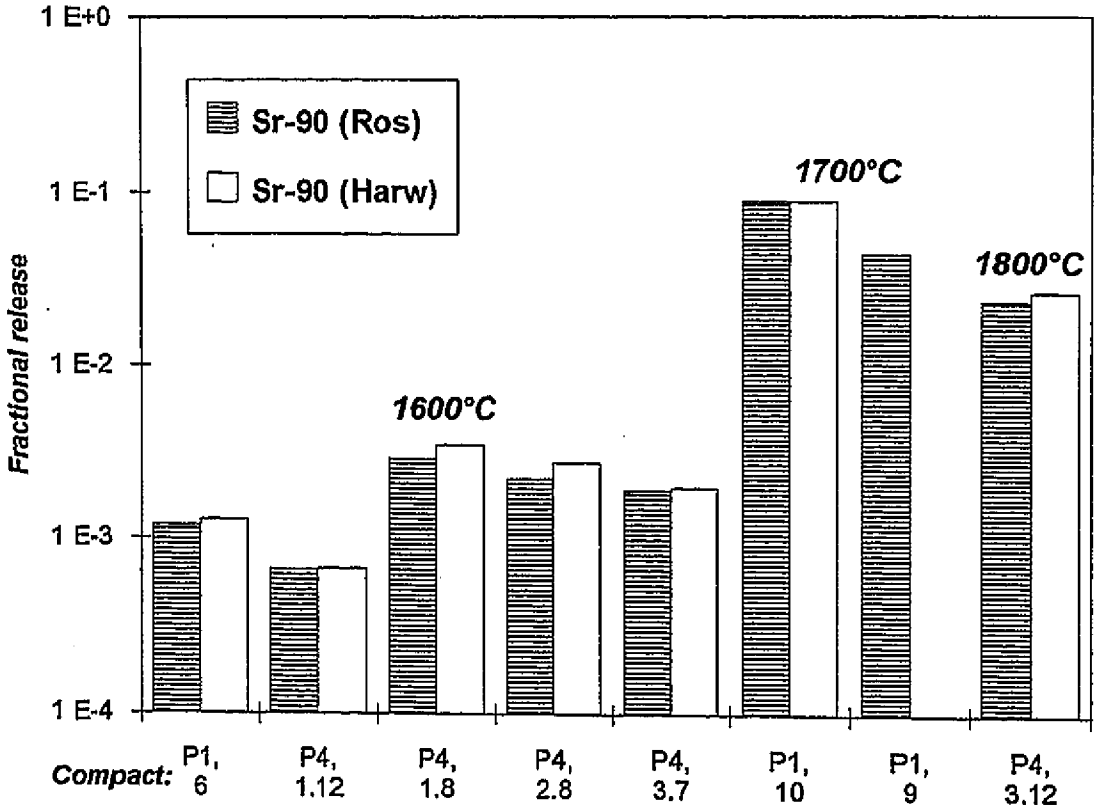

Fig. 28: ^{90}Sr fractions in the matrix graphite after heating tests of HFR-P4 and SL-P1 compacts - comparison between Harwell and Rossendorf measurements

After the 1700°C test, the ^{90}Sr concentrations in the matrix graphite are one to two orders of magnitude higher than at 1600°C. This shows that at 1700°C ^{90}Sr diffuses relatively rapidly through particle coatings which are still gastight (Fig. 25). At 1800°C, the ^{90}Sr concentration is lower than at 1700°C, due to the faster release from the compact.

Fig. 29 shows a comparison of the ^{137}Cs values obtained at Harwell and Jülich. In contrast to ^{90}Sr, the ^{137}Cs fraction in the matrix graphite rises at 1800°C. However, the jump from the similarly low values at 1600°C to 1700°C is clearly greater than from 1700 to 1800°C.

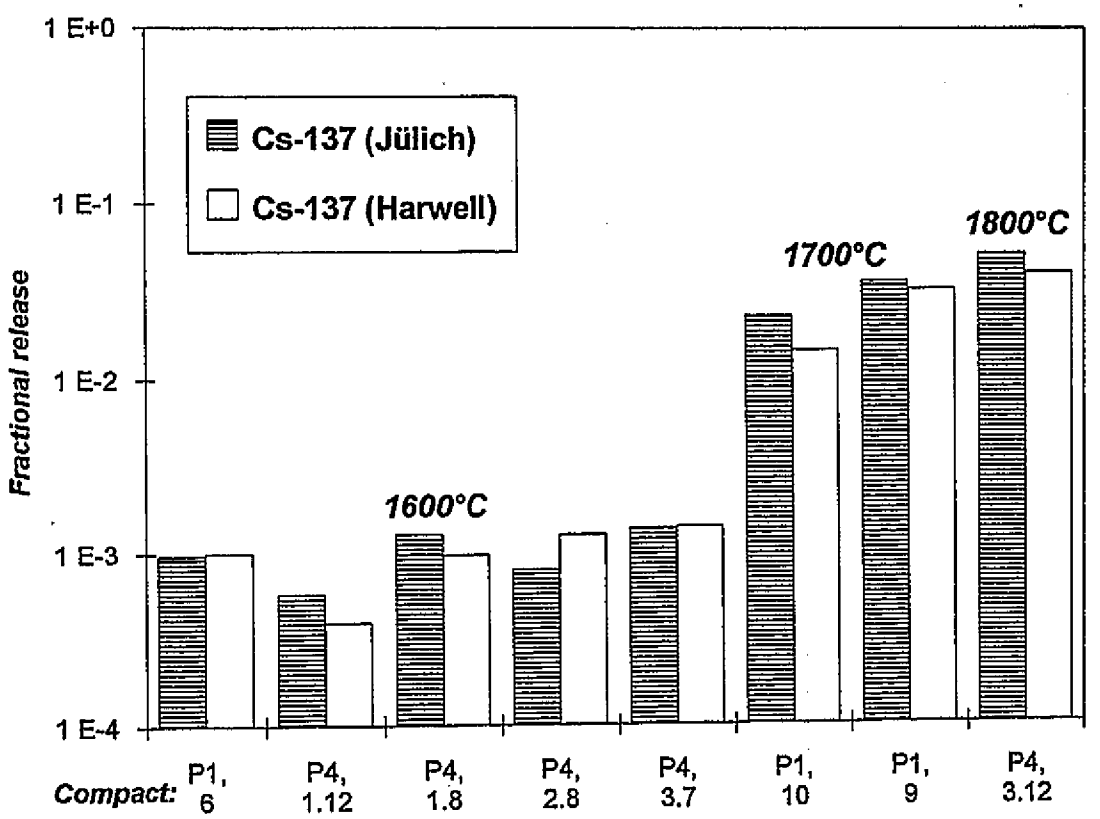

Fig. 29: ^{137}Cs fractions in the matrix graphite after 300 h heating tests of HFR-P4 and SL-P1 compacts
- comparison between Harwell and Jülich measurements.

On the whole, the agreement between the Harwell and Jülich values may be regarded as satisfactory even if an individual value deviates by 60 % HFR-P4/2/8 and the overall variation is 16 %.

6.5 Fission product transport and particle deterioration

After deconsolidating the heated compacts, ten particles each were removed to determine the fission product distribution. The particles were first measured individually by gamma spectrometry. Then each particle was cracked, the kernel and coating separated and subsequently also measured /51/.

Even after the 1800°C experiment the fission products ^{106}Ru, ^{144}Ce and ^{154}Eu were found almost completely in the fuel kernels. A release of about 50 to 70 % from the kernels into the coating was measured for ^{125}Sb in the particles heated at 1700 and 1800°C. At 1600°C, with one exception (SL-P1, 6), antimony was completely retained in the kernels. No measurements were carried out to detect strontium.

The ^{134}Cs and ^{137}Cs activity was easily measurable in all samples. The average values of the fractions relative to the inventory at the end of irradiation determined from 10 or 9 measurements respectively are compiled in Tab. 18.

UO2-TRISO Compact	*Heating Temp. (°C)*	***Fractional Cs-137 content***				
		Kernel	***Coating***	***Particle***		
				Measurem.	*Standard dev.**	*Calculated ***
SL-P1, 6	1600	0.10	0.90	0.96	0.07	1.00
HFR-P4, 1.12	1600	0.03	0.97	0.84	0.15	1.00
HFR-P4, 1.8	1600	0.10	0.90	0.87	0.14	1.00
HFR-P4, 2.8	1600	0.09	0.92	0.88	0.05	1.00
HFR-P4, 3.7	1600	0.15	0.85	0.89	0.22	0.99
SL-P1, 10	1700	0.03	0.76	0.80	0.25	0.86
SL-P1, 9	1700	0.05	0.75	0.80	0.11	0.88
HFR-P4, 3.12	1800	0.02	0.28	0.30	0.27	0.43

* Standard deviation of measured values of 9 or 10 particles, respectively

** Extrapolated to a total of 100% including release from particles

Table 18: Average fractions of ^{137}Cs in 10 (9) particles from compacts after heating tests at 1600, 1700 or 1800° C

It is apparent that the release from the kernels is very high even at 1600°C. Although caesium is almost completely retained in the coating in the 1600°C heating tests, a significant release from the particles begins at 1700°C /52/. In all cases, the average measured particle inventories are below the individual values calculated from the compact measurements. This systematic error of about 10 % remains within a satisfactory margin. The individual measurements of the particles from the three compacts heated at different temperatures are shown diagrammatically in Fig. 30. It becomes clear that the release from the kernels into the coatings and also through the coatings from the particles differs individually. This behaviour, which was also observed for particles from heated spherical fuel elements /40, 53/, may be essentially attributed to statistical variations typical of ceramic materials.

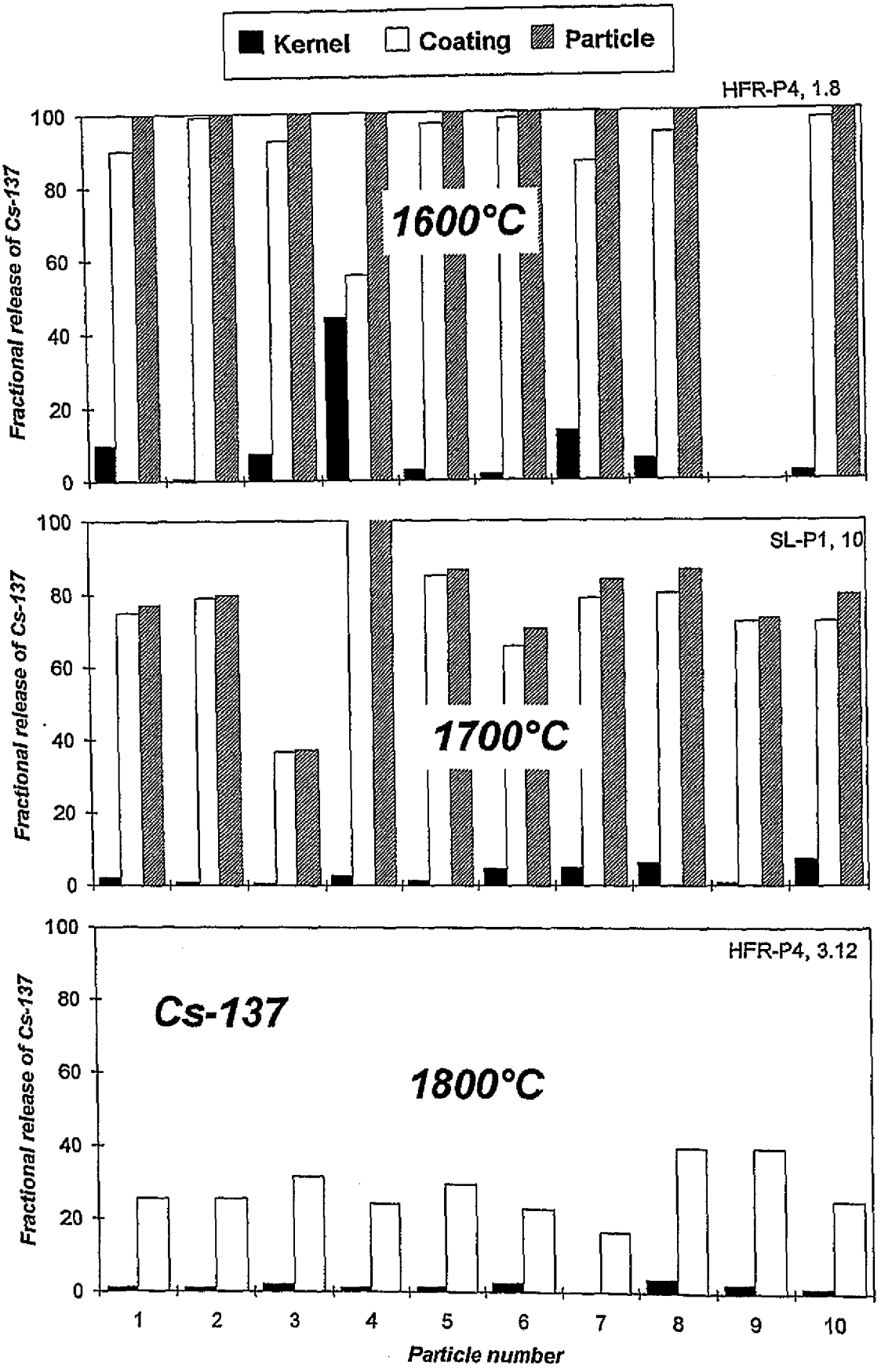

Fig. 30: ^{137}Cs distribution in coated particles from compacts after isothermal heating for about 300 hours

Figs. 31 to 36 show ceramographic sections of particles from heated compacts /54/. It can be seen from Fig. 31 that the kernel is greatly changed with increasing burnup. Large pores influencing the transport behaviour of fission products arise at higher burnups as a consequence of the growing fission gas inventory and the oxygen released during the fission of UO_2. The enlarged coating sections of particles from compacts with 11 and 14 % fima respectively heated at 1600°C (Fig. 32) show changes in the SiC layer starting from the inside in particles with higher burnup. The black spots in the bright SiC layers are due to surface fracture which occurs during ceramographic grinding if preceded by embrittlement of the SiC. Microprobe examinations of particles from heated fuel elements in connection with ceramographic and gamma spectrometric investigations have shown that in particular a relation can be established between caesium diffusion and embrittlement in the SiC /40, 55/. The fact that in the 50 µm thick SiC layer, caesium diffusion is more advanced than for particles with the same high burnup with 35 µm can be attributed to individual differences in the particles and not to the different quality of the SiC layers, as also shown by the other results. As the measurements show (Fig. 30), caesium diffused through the coatings at 1700°C. Consequently, black dots can be recognized over the entire SiC thickness in Fig. 33. Due to the start of annealing, embrittlement of the SiC is reduced at 1800°C and also the surface peeling during grinding.

As a consequence of the annealing at 1800°C, the pores in the fuel kernels have become enlarged thus causing the kernels to swell entailing a densification of the buffer layer (light ring immediately surrounding the kernel) (Fig. 34). The fact that greater changes tend to be determined for particles from SL-P1 compacts may possibly be attributed to the lower irradiation temperatures and thus smaller annealing effects and poorer flow behaviour of the PyC in the SL-P1 experiment in comparison to HFR-P4. Figs. 35 and 36 both show on the right hand side particles with cracked kernels and radial cracks in the buffer layer. Cracking of the buffer layer is due to kernel swelling and simultaneous shrinkage of the pyrolytic carbon during irradiation. In contrast, radial cracks in the SiC layer can be attributed to sample preparation and tend to occur with more brittle material.

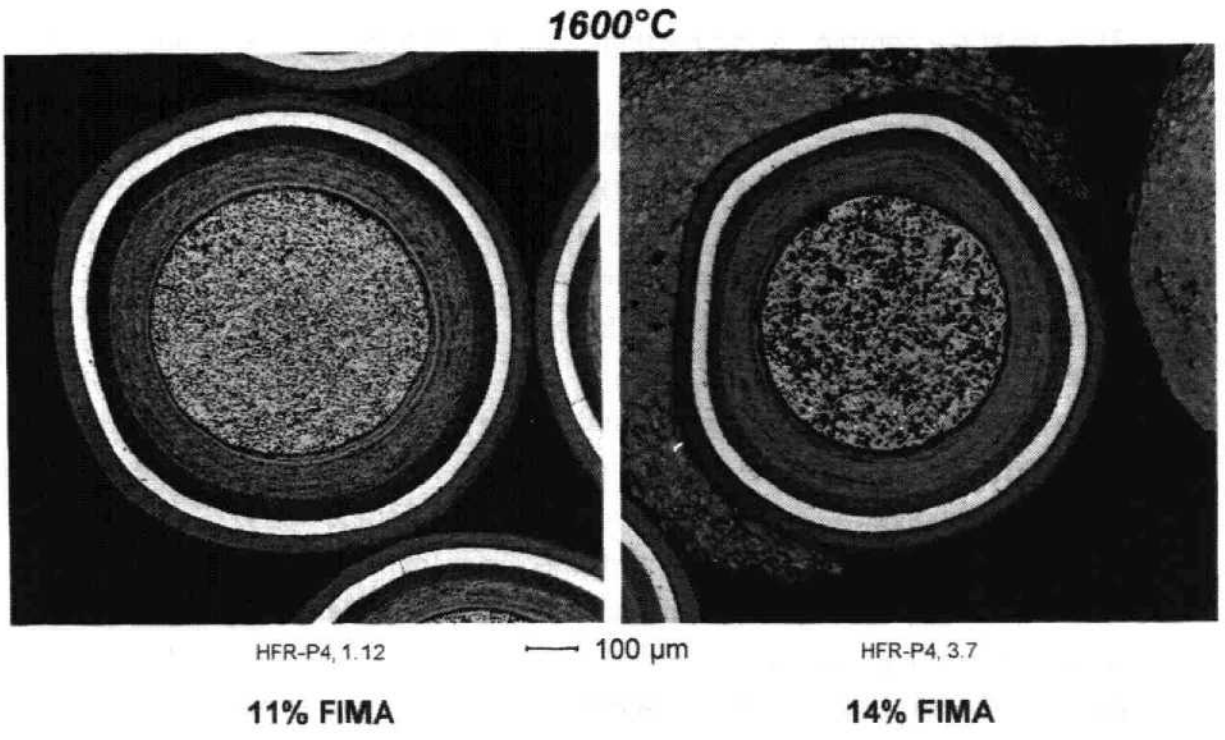

Fig. 31: Ceramographic sections through particles from compacts with different burnup heated for 304 hours at 1600° C

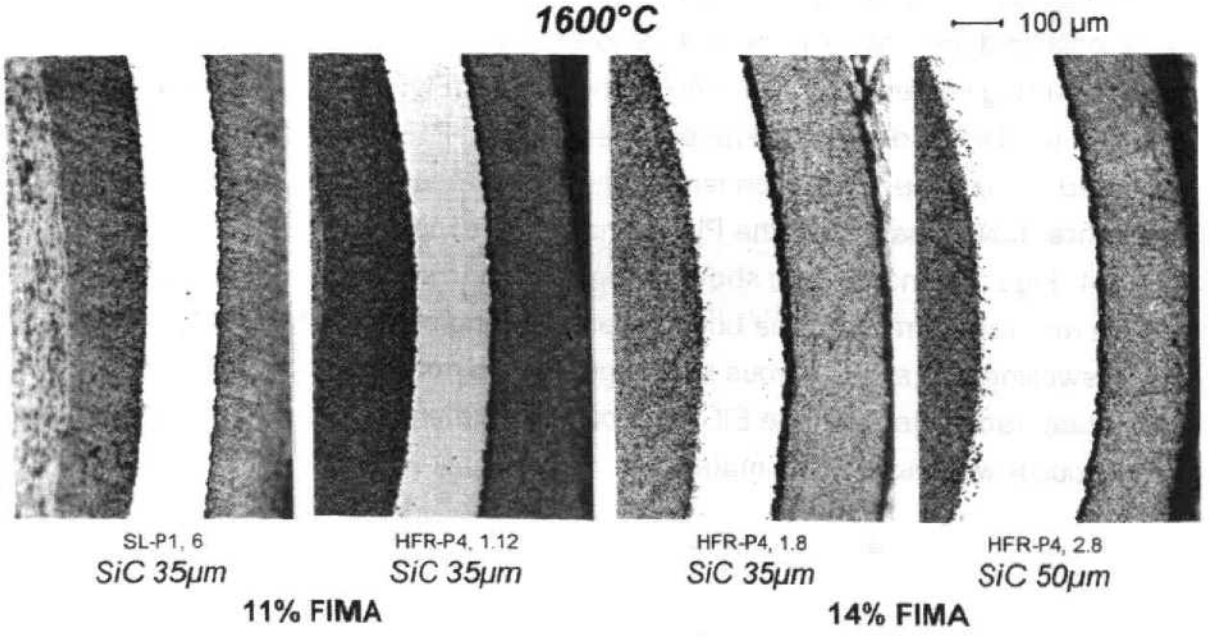

Fig. 32: Ceramographic sections through coating segments of particles - in one case with a thicker SiC layer - from compacts of two burnup classes after 304 hours at 1600° C

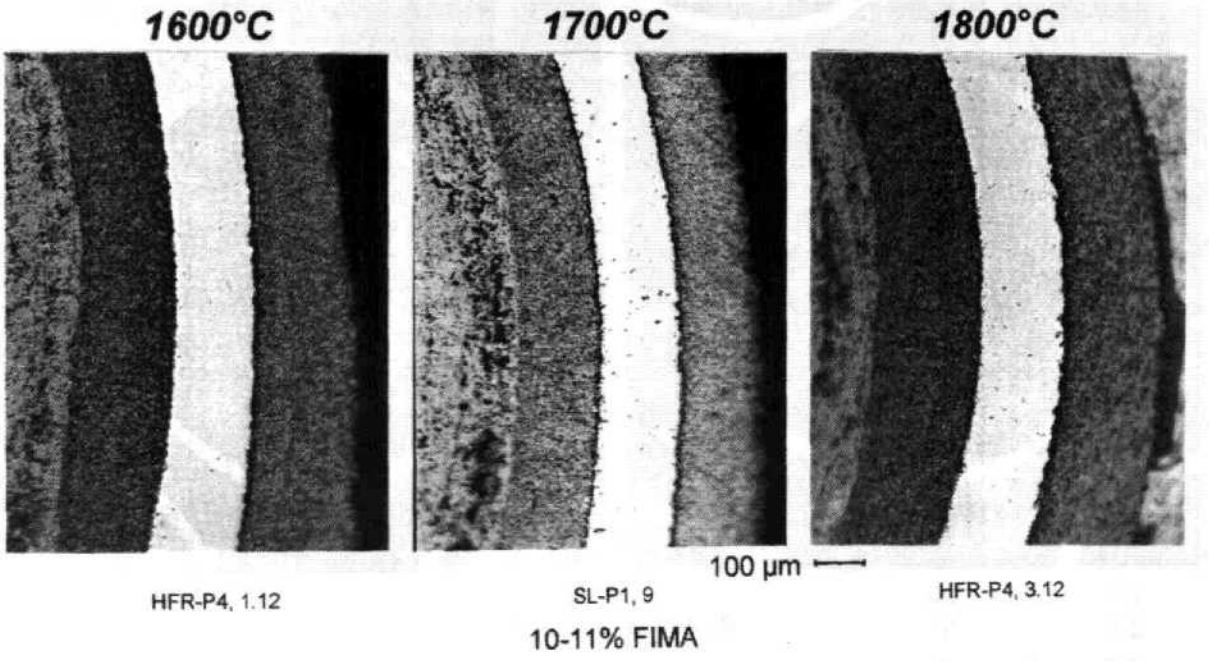

Fig. 33: Ceramographic section through coatings from compacts heated of 1600, 1700 or 1800° C

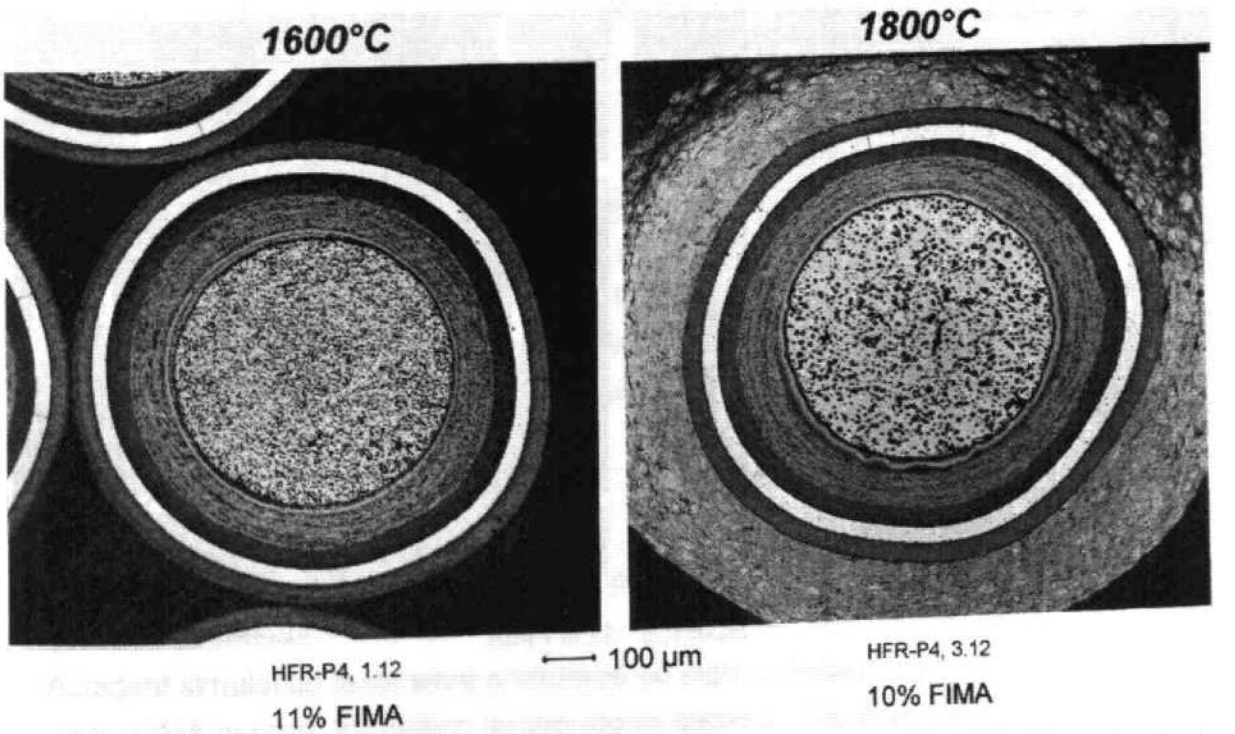

Fig. 34: Particles from compacts heated for 304 hours at 1600° C and 279 hours at 1800° C

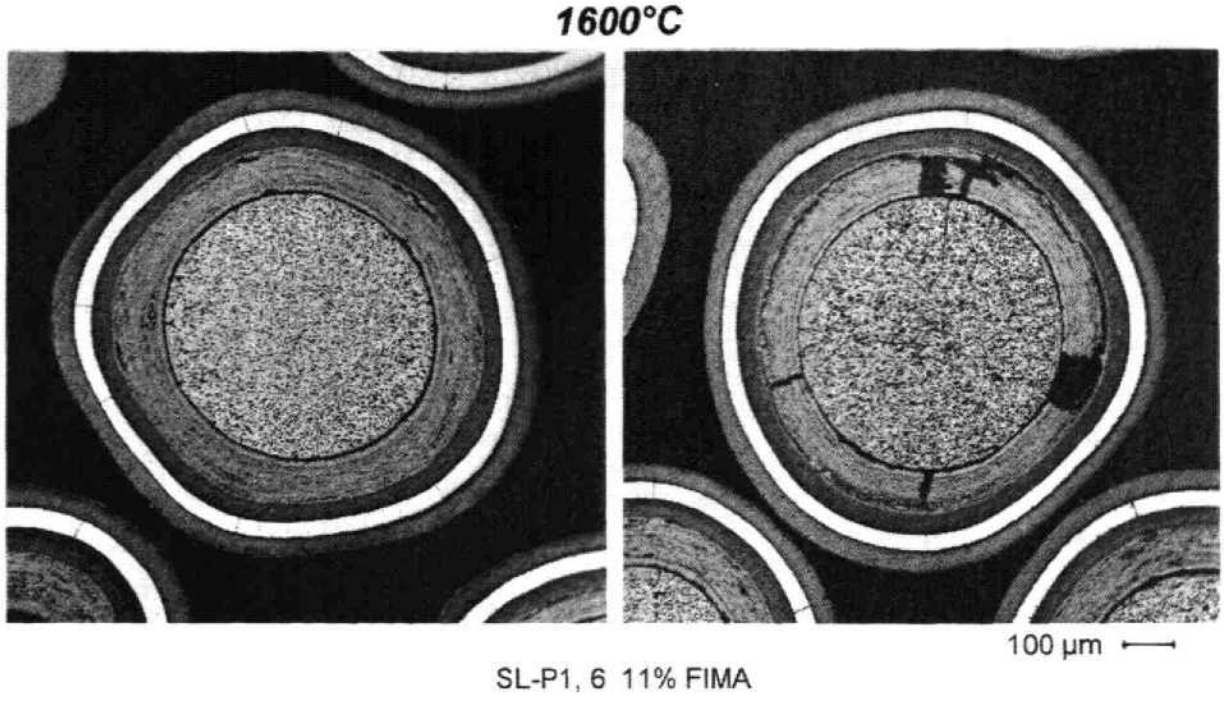

Fig. 35: Particles from a compact heated for 304 hours at 1600° C

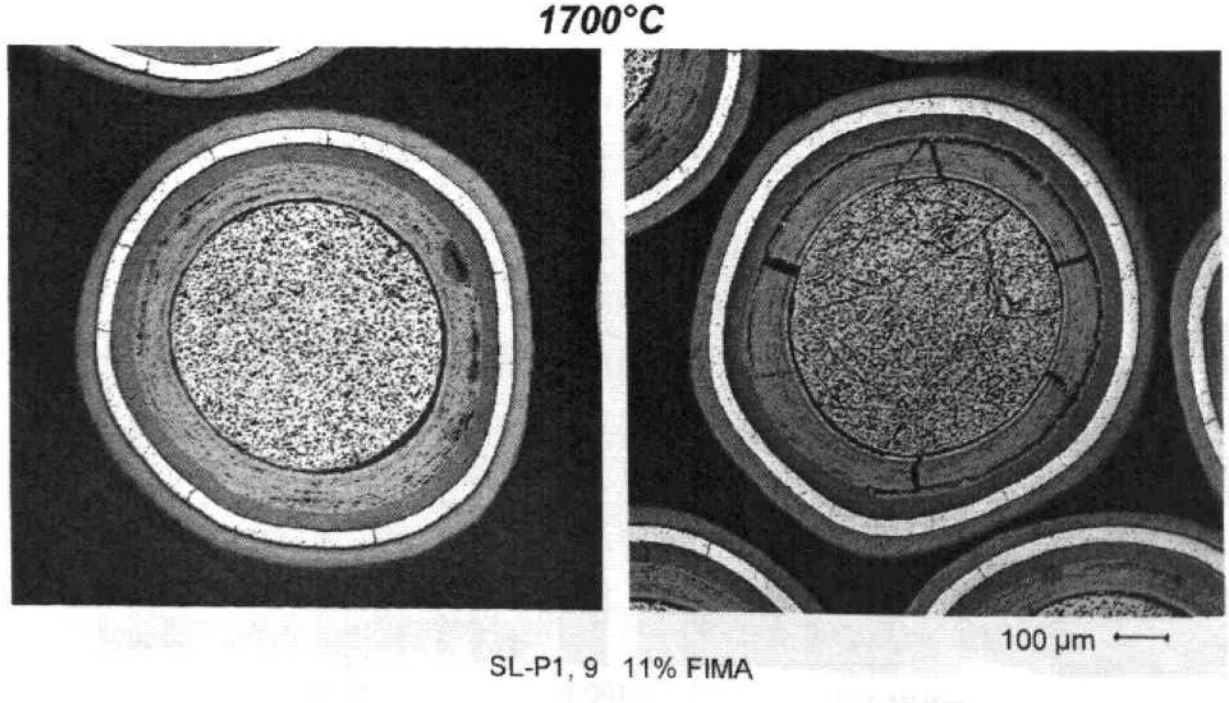

Fig. 36: Particles from a compact heated for 304 hours at 1700° C

Ten or nine particles respectively from each compact were crushed and the force-path diagram plotted under defined conditions. Whereas the path length did not display any interpretable changes, the force necessary for crushing becomes significantly smaller with increasing heating temperature (Tab. 19). It is striking that the 1700°C values of particles from the two SL-P1 compacts are below those at 1800°C in the HFR-P4 compact. The reason might be the greater damage to the kernels and buffer layers in the SL-P1 particles determined by the ceramographic investigations.

Fuel compact	*SiC layer (µm)*	*Burnup (%FIMA)*	*Fast fluence 1E+25 1/m² (E>16 fJ)*	*Irradiation temperature (°C)*	*Heating temperature (°C)*	***Crushing Strength (N)***
SL-P1, 6	36	10.7	6.7	790	1600	**19.2**
HFR-P4, 1.12	36	11.1	5.5	900	1600	**19.3**
HFR-P4, 1.8	36	13.8	7.2	900	1600	**19.5**
HFR-P4, 2.8	51	13.8	7.2	900	1600	**19.3**
HFR-P4, 3.7	36	13.9	7.5	1050	1600	**19.7**
SL-P1, 10	36	10.3	6	790	1700	**15.0**
SL-P1, 9	36	10.7	6.3	790	1700	**14.2**
HFR-P4, 3.12	36	9.9	5.5	1050	1800	**15.5**

Table 19: Average crushing strength of 10 (9) particles from heated compacts

In experiments on particles with similar SiC coating - but mixed oxide kernels - forces of about 21 N were necessary for crushing after irradiation to similarly high burnups and fast neutron fluences. The 1600°C results are relatively close to these values whereas in the case of the particles heated to 1700°C a clear loss of strength occurred, which can be attributed to a deterioration of SiC due to fission product transport.

6.6 Summarizing evaluation of the results

Accident simulation tests were performed on eight compacts with about 11 or 14 % FIMA burnup, irradiation temperatures between 790 and 1050°C and high fast neutron fluences of 5.5 to 7.5 x $10^{25}m^{-2}$ (MODUL values: 9 % FIMA, 840°C,

2 x $10^{25}m^{-2}$ for E > 16 f J). The target temperatures of 1600, 1700 and 1800°C were maintained for about 300 hours.

a) Fission gas/iodine release

In all cases, it was only possible to measure the ^{85}Kr release whereas the highly active iodine nuclides of significance for accident impacts had completely decayed at the time of the experiments. Nevertheless, it has been repeatedly demonstrated with the same fuel - under similar conditions - that the fission gas and iodine releases are almost identical /40, 57/. Fig. 37 gives an overview of ^{85}Kr release.

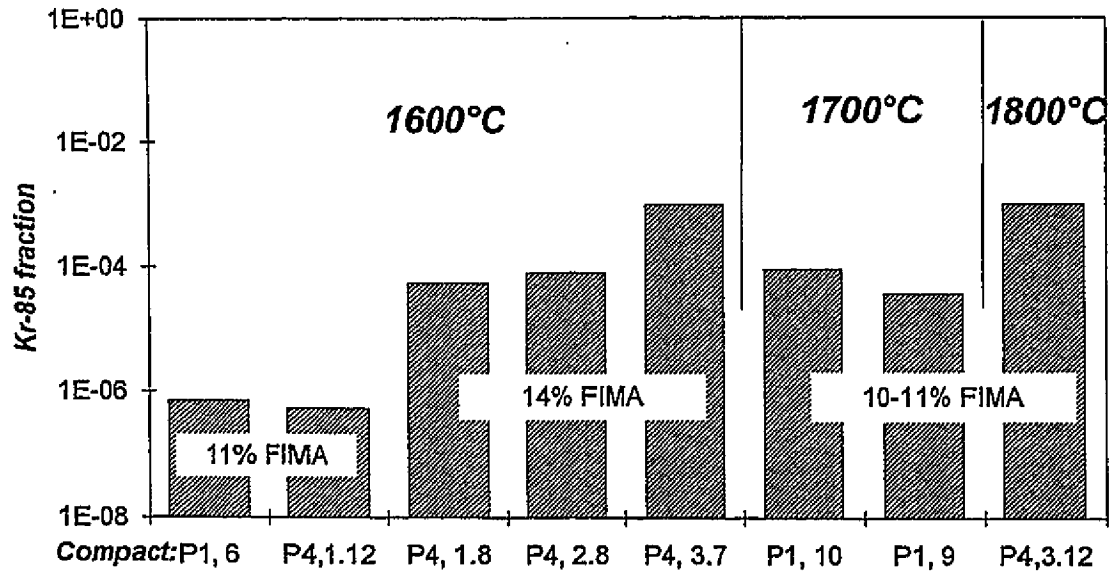

Fig. 37: ^{85}Kr release during 300 h heating tests from compacts of the HFR-P4 and SL-P1 irradiation experiments

In two experiments with compacts at 1600°C with 11 % FIMA burnup, gas release remains very low because no damage at all occurred at the particle coatings. In the case of the three compacts with high burnup, however, ^{85}Kr releases were achieved at 1600°C similar to those in the 1700 and 1800°C experiments. Under these conditions the structure of the SiC layer is altered as a consequence of the diffusion of solid fission products (caesium, strontium) which also leads to permeability for fission gases. However, the intact layers of pyrocarbon prevent a significant release. Only in the case of HFR-P4/3/7 with the most severe irradiation conditions was a particle damaged after about 50 hours at 1600°C by pressure vessel failure.

b) Caesium release

After iodine, the greatest significance for accident impacts in a small HTR is attributed to the caesium nuclides /58/. The most extensive results are available about caesium distribution and release from the compacts; these results are compiled in Table 20 and shown in Fig. 38. In particles from the compacts heated at 1600°C the released fraction is small so that the values were normalized to a fraction of 100 %. In contrast, for the compacts heated at 1700 and 1800°C the values are given relative to the ^{137}Cs inventory measured before the experiments. Adding up the values of the individual components and the released fraction should similarly result in 100 %. However, it is apparent that measuring errors led to a total on average about 10 % lower, which may be regarded as a satisfactory result. The values were also normalized to 100 % in Fig. 38. The Figure shows the high caesium release from the kernels in all experiments. Whereas at 1600°C the retention in the particles is practically still complete, a significant release of caesium takes place at 1700°C within the heating time of 304 hours, which is greatly increased at 1800°C. In comparison to the heating experiments with spherical fuel elements at 1800°C for 100 or 200 hours, the fractions in the matrix graphite are low /40, 43/.

UO2-TRISO Compact	*Heating temp. (C°)*	*Average Cs-137 content in*				*Fract. Cs-137 release from compact*	*Total Cs-137*
		Kernel *	*Coating* *	*Particle*	*Matrix*		
SL-P1, 6	1600	9.7%	90.2%	99.9%	0.1%	0.0%	100%
HFR-P4, 1.12	1600	3.3%	96.6%	99.9%	0.1%	0.0%	100%
HFR-P4, 1.8	1600	9.9%	89.8%	99.7%	0.1%	0.2%	100%
HFR-P4, 2.8	1600	8.5%	91.3%	99.8%	0.1%	0.1%	100%
HFR-P4, 3.7	1600	14.8%	84.7%	99.5%	0.1%	0.4%	100%
SL-P1, 10	1700	3.3%	76.3%	79.6%	2.3%	10.4%	92.3%
SL-P1, 9	1700	4.7%	75.0%	79.7%	3.6%	9.8%	93.1%
HFR-P4, 3.12	1800	1.8%	28.1%	29.9%	5.2%	52.3%	87.4%

* Fraction in 10 or 9 particles, respectively

Table 20: ^{137}Cs fractions in compacts after heating tests

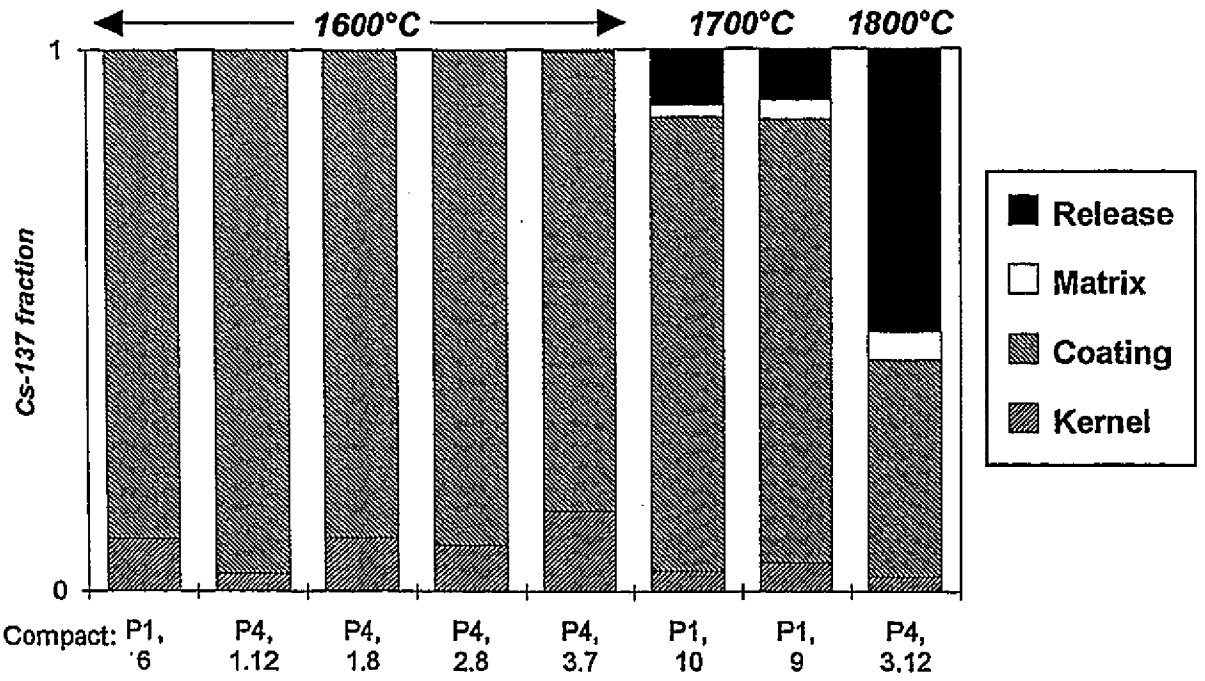

Fig. 38: ^{137}Cs fraction in and release from compacts of experiments HFR-P4 and SL-P1 after about 300 hours of isothermal heating

c) Strontium release

As examinations of particles from heated fuel elements have shown, in comparison to caesium, strontium is retained significantly more effectively in the fuel kernels and matrix graphite at 1600°C /40, 43/. Therefore, the release from the compacts at 1600°C is also lower than that of caesium. At 1700 to 1800°C, the strontium release approaches that of caesium.

d) Silver release

Of all the fission products, silver is released most rapidly. Due to the small inventory and short half-life in comparison to ^{137}Cs and ^{90}Sr, it is of less significance for accident consequences and was therefore only measured in one experiment.

e) Release of other fission products

Apart from ^{134}Cs and ^{137}Cs, other fission products were also measured in the gamma spectrometric investigations of the compact components. ^{106}Ru, ^{144}Ce and ^{154}Eu were almost completely retained in the fuel kernels even at 1800°C. With its low formation rate, 50 to 70 % of the ^{125}Sb inventory was released from the kernels into the coating at 1700 and 1800°C. In the matrix graphite of the compacts heated at 1700 and 1800°C only ^{106}Ru and ^{154}Eu were measured at 1 %.

7. Conclusions:

- Modern UO_2 TRISO fuel has excellent performance under expected HTR MODUL conditions, and also under more-extreme conditions:

HTR MODUL	HFR-P4 max. values
$2.1 \times 10^{25} m^{-2}$	$8 \times 10^{25} m^{-2}$ fluence
9% FIMA	15% FIMA burnup

- In general, both SiC and PyC coating layers are important in obtaining high fuel performance, and modern TRISO fuel had no "pressure vessel" failure of coatings during normal reactor irradiation. Only very limited pressure vessel failures occurred during post-irradiation heating tests.

- The dominating influence on TRISO fuel performance is burnup - assuming that irradiation temperatures are around 1000°C in HTRs. With burnup, the fission product concentration increases at the inner SiC surface which may lead to a degradation of this most important fission product retaining layer.

- During reactor irradiation, the release rates of short-lived fission gases from the fuel were maintained at very low levels by the integrity of the fuel particles and were only from contamination. Fission gases are representative of iodine.

- Early gas release fractions during accident condition testing were low at $<10^{-6}$, even at 1800°C for 50h. With ≤11% FIMA fuel, release remains at this low level throughout the 1600°C tests. With 14% FIMA fuel at 1600°C, pressure vessel failure leads to 10^{-3} fractional release of ^{85}Kr after 300 h. At 1800°C, 10^{-3} release fractions are reached as a consequence of diffusion through degraded SiC. Whenever solid fission product release is increasing, krypton is further delayed by still intact pyrocarbons.

- HFR-P4 and SL-P1 saw only one year irradiation, but results are consistent with 500-600 day irradiation tests in HFR and FRJ2 and with results obtained from AVR elements with more than 2000 day irradiation.

- On the available evidence of accident conditions testing, fission products are retained up to the "1600°C" limit and possibly even higher - as long as 11% FIMA is not exceeded. With UO_2 TRISO fuel irradiated to 14% FIMA, this type of fission product retention can be strictly only guaranteed up to 1600°C.

8. References

/1/ G. Lohnert

Technical design features and essential safety-related properties of the HTR-module
Nucl. Eng. Des. 121 (1990), 259

/2/ T. Haque and H. Werner

AVR-Versuchsprogramm: HTA-5-Kühlmittelverluststörfall
Siemens-INTERATOM Note No. 54.07907.5, January 1990

/3/ W. Rehm, J. Cleveland and T. Iyoku

Thermodynamic Investigations of Loss-of-Coolant Accidents for HTGRs based on AVR Simulation Experiments
ASME/AICKE Conf. on Thermal Hydraulics, San Diego, August 1992

/4/ K. Krüger, A. Bergerfurth, S. Burger, P. Pohl, M. Wimmers and J. C. Cleveland

Preparation, conduct and experimental results of the AVR loss-of-coolant accident simulation test
Nucl. Sci. Eng. 107 (1991), 99

/5/ W. Kröger, J. Wolters, J. Mertens, R. Moormann, W. Rehm

Preliminary Results of an Updated Probalistic Safety Analysis for the German HTR-MODUL
Proc. 2nd Post SMiRT Seminar on Small and Medium-Sized Nuclear Reactors, San Diego, August 1989

/6/ H. Nickel

Entwicklung von beschichteten Brennstoffteilchen
KFA-Report, Jül-687-RW, August 1970

/7/ H. Ragoß, W. Heit, H. Nabielek, W. Schenk

Absicherung der brennelementspezifischen Quelltermine für die radiologische Auslegung des HTR-MODUL
Jahrestagung Kerntechnik '88, Tagungsbericht p. 461, May 1988

/8/ H. Nabielek, W. Kühnlein, W. Schenk, W. Heit, A. Christ and H. Ragoß

Development of advanced HTR fuel elements
Nucl. Eng. Des. 121 (1990), 199

/9/ H. Nabielek,, W. Schenk, K. Verfondern

Quantitative Evaluation of the Performance of German HTR Fuel under Normal Operating and Accident Conditions
KFA-ISR-IB-19/93, Dec. 1993

/10/ G. H. Lohnert, H. Nabielek, W. Schenk

The Fuel Element of the HTR-Module, a Prerequisite of an Inherently Safe Reactor SMiRT Post-Conf. Seminar on Small and Medium-Sized Nuclear Reactors, Lausanne, Aug. 24-26, 1987

/11/ R. Gontard and H. Nabielek

Performance Evaluation of Modern HTR TRISO Fuels
Research Centre Jülich Internal Report KFA-HTR-IB-05/90, July 1990

/12/ W. Schenk, H. Nabielek, G. Pott, H. Nickel

Die Spaltproduktrückhaltung im Brennelement
Fortschritte iin der Energietechnik, p. 321, Forschungszentrum Jülich, 1993

/13/ R. Duwe, W. Kühnlein, R. Schröder

Gamma-spektrometrische Abbrandmessungen an kugelförmigen Brennelementen
KFA-Report, Jül-1428, June 1977

/14/ W. Schenk, D. Pitzer and H. Nabielek
Fission product release profiles from spherical HTR fuel elements at accident temperatures
Report Jül-2234, Research Centre Jülich (1988) (Jül-2091 in German)

W. Schenk and H. Nabielek

Kugelbrennelemente mit TRISO-Partikeln bei Störfalltemperaturen (Zahlenwerk zum Bericht Jül-2091 und neue Ergebnisse von 1986 bis Oktober 1988)
Report Jül-Spez-487, Research Centre Jülich (1989)

/15/ R. Conrad, A.-W. Mehner, G. Pott

Bestrahlungserprobung und Auswertung für HTR-LEU-Referenzbrennelemente im HFR Petten
Jahrestagung Kerntechnik '83, Berlin, Tagungsbericht p. 621, June 1983

/16/ R. Gontard, A.-W. Mehner, H. Jünemann

Vorbestrahlungsbericht für das Experiment HFR-P4
KFA-HBK-IB-17/91, Dec. 1991

/17/ R. Gontard, A.-W. Mehner

Vorbestrahlungsbericht für das Bestrahlungsexperiment SILOE-P1
KFA-HBK-IB-17/82, Dec. 1982

/18/ W. Burck, P. Krautwasser

Datensatz zum Bestrahlungsverhalten von hochangereicherten (Th,U)-Mischoxid-Brennstoffteilchen mit SiC-Zwischenschicht (LTI-TRISO-Partikeln)
KFA-IRW-IB-13/88, July 1988

/19/ K. Bongartz, E. Gyarmati, H. Schuster, K. Täuber

The Brittle Ring Test: A Method for Measuring Strength and Young's Modules on Coatings of HTR Fuel Particles
J. Nuc. Mat. 62, p. 123, 1976

/20/ W. Heit, H. Huschka, G. Kaiser, W. Rind

Status of Qualification of High-Temperature Reactor Fuel Element Spheres
Nuclear Technology, Vol. 69, p. 44, April 1985

/21/ H.-J. Hantke

Performance of High Quality HTR-LEU Fuel Elements with TRISO Coated Particles
KFA-HTA-IB-7/92, Dec. 1992

/22/ M. Kadner, J. Baier

Über die Herstellung von Brennstoffkernen für Hochtemperaturreaktor-Brennelemente
Kerntechnik, Vol. 18, 1976, No. 10

/23/ R. Conrad

Irradiation of Low Enriched Uranium Reference HTR Coated Fuel Particles at 1000°C and 1200°C for Failure Rate Examination in the HFR Petten,
Project D 175.01/02/03
Design and Safety Report, April 1982

/24/ J. Gentil

Experience SILOE-P1, Contrat GR 761306, Description (Assemblierungsbericht)
Pi/SEDTI/486/82/GJ/cc, 2 August 1982

/25/ C. de Bagneaux

Note Technique de Securite-Dispositif "TUMULT"
PI No 80-23, 1 February 1980

/26/ R. Conrad, G. Robert

Manual for Sweep Loops
Technical Memorandum IT/80/1679, July 1980

/27/ R. Gontard, A.-W. Mehner, private communication, Feb. 1981

(Herstellung, Charakterisierung und Aktivierungstest der Bestrahlungsproben für das Experiment SILOE-P1 (HEU-Brennstoff)
HBK-TN-5/81, February 1981)

/28/ K. Kugeler, R. Schulten
Hochtemperaturreaktortechnik
Springer-Verlag, 1989

/29/ W. Schenk, A. Naoumidis, H. Nickel

The Behaviour of Spherical HTR Fuel Elements under Accident Conditions
Journal of Nucl. Mat. 124, p. 25, 1984

/30/ W. Schenk and H. Nabielek

Kugelbrennelemente mit TRISO-Partikeln bei Störfalltemperaturen (Zahlenwerk zum Bericht Jül-2091 und neue Ergebnisse von 1986 bis Oktober 1988)
Report Jül-Spez-487, Research Centre Jülich (1989)

/31/ H. Reutler, G. H. Lohnert

Advantages of Going Modular in HTR
Nuclear Engineering and Design, Vol. 78, No. 2, April 1984

/32/ K. Verfondern, R. C. Martin, R. Moormann

Methods and Data for HTGR Fuel Performance and Radionuclide Release Modeling during Normal Operation and Accidents for Safety Analysis
Report Jül-2721, Jan. 1993

/33/ W. Schenk and H. Nabielek

High-Temperature Reactor fuel fission product release and distribution at 1600°C
Nucl. Techn. 96 (1991), 323

/34/ W. Schenk, G. Pott and H. Nabielek

Fuel performance testing for small HTRs
J. Nucl. Mater. 171 (1990), 235

/35/ H. Nabielek, H. Nickel, G. Pott, W. Schenk

Development and Qualification of Modern TRISO Fuels for the HTRs
Research Coordination Meeting, IAEA Vienna, 23-25 June 1993

/36/ W. Schenk, H. Nabielek

Testing of irradiated spherical fuel elements at HTR MODUL relevant accident conditions
IAEA Specialist Meeting on Behaviour of Gas Cooled Reactor Fuel under Accident Conditions
Oak Ridge, USA, 5.-8. Nov. 1990

/37/ G. Behrens, G. Schürer

Private communication 27.07.1988
/IRW-TN-57/88)

/38/ K. Landsgesell, H. Dahmen, W. Kühnlein, R. Schröder

Private communication 05.12.89 and 11.06.90
(IRW-TN-116/89 and -29/90)

/39/ A.-J. Inns, J. G. Henley

Post irradiation Examination of Electrolyte and Graphite Samples from Selected HTR Specimens
AEA-FS-0084 (H), Sept. 1991

/40/ B. Gleisberg, M. Böttger

Private communication, Sept. 1991

/41/ W. Landsgesell, H. Dahmen, W. Kühnlein, R. Schröder

Private communication 13.12.90, 14.02.91
(IRW-TN-18/91)

/42/ K. Fukuda, K. Hayashi, K. Shiba

Fuel Behaviour and Fission Product Release under HTGR Accident Conditions
International Seminar on "Fission Product Transport Processes in Reactor Accidents" Dubrovnik, Yugoslavia (May 22-26, 1989) by International Centre for heat and mass transfer
proc: Hemisphere Publ. Coop., p. 197, 1990

/43/ G. Reitsamer, J. Zeger, G. Stolba, G. Falta

Nachbestrahlungsuntersuchungen aus der geglühten Kugel 14 aus dem Experiment R2-K13
OEFZS-A-1106, CH-380/87, Nov. 87

/44/ H. Derz, T. Floßdorf

Private communication 16.11.1990
(IRW-TN-79/90)

/45/ P. Brown, A. Inns, R. J. Patermann, B. A. Philips, B. M. Sharpe

Post-Irradiation Examination of HTR Fuel Elements AVR 76/20, 72/22, 74/11, HFR-K3/1, HFR-K3/3, FRJ2-K13/2
A.E.R.E. -64740, Aug. 1988

/46/ K. Landsgesell, H. Dahmen, W. Kühnlein, R. Schröder

Private communication 15.03. und 05.07.1990
(IRW-TN-14/90)

/47/ W. Schenk, H. Nabielek

Iodine Retention in Spherical Fuel Elements under HTR MODUL Accident Conditions Annual Meeting on Nuclear Technology '90, Nürnberg
Proceedings, p. 363, May 1990

/48/ G. Breitbach et al.

Sicherheitstechnische Untersuchungen zum Störfallverhalten des HTR-MODUL
KFA-Report, Jül-Spez-335, Nov. 1985

FORSCHUNGSZENTRUM JÜLICH GmbH

KFA

Jül-2992
November 1994
ISSN 0944-2952